

LMSC D501627

THE LOCKHEED ALTERNATE
PARTIAL POLARIZER UNIVERSAL FILTER

Alan M. Title
Lockheed Palo Alto Research Laboratory
3251 Hanover Street
Palo Alto, California 94304

March 1976

Final Report for Period October 8, 1974
October 8, 1974 - October 7, 1975

Prepared for
GODDARD SPACE FLIGHT CENTER
Greenbelt, Maryland 20771

TECHNICAL REPORT STANDARD TITLE PAGE

1. Report No.		2. Government Accession No.		3. Recipient's Catalog No.	
4. Title and Subtitle The Lockheed Alternate Partial Polarizer Universal Filter				5. Report Date March 1976	
7. Author(s) Alan M. Title				8. Performing Organization Report No. LMSC D501627	
9. Performing Organization Name and Address Lockheed Palo Alto Research Laboratory 3251 Hanover Street Palo Alto, CA 94304				10. Work Unit No.	
12. Sponsoring Agency Name and Address National Aeronautics and Space Administration Goddard Space Flight Center Greenbelt, Maryland 20771				11. Contract or Grant No. NAS5-20783	
				13. Type of Report and Period Covered Final Report October 8, 1974 - October 7, 1975	
15. Supplementary Notes				14. Sponsoring Agency Code	
16. Abstract A tunable birefringent filter using the alternate partial polarizer (APP) design of Title has been built. The filter has a transmission of 38% in polarized light. Its full width at half maximum is .09 μ at 5500 \AA . It is tunable from 4500-8500 \AA by means of stepping motor actuated rotating half wave plates and polarizers. Wave length commands and thermal compensation comands are generated by a PPD 11/10 mini computer. In Section I the Lockheed Alternate Partial Polarizer Universal Filter is compared with the Zeis Universal Birefringent Filter. In Sections II, III and IV the design, techniques, construction methods, and filter performance are discussed in some detail. Based on the experience of this filter some conclusions regarding the future of birefringent filters are discussed in Section V.					
17. Key Words (Selected by Author(s)) Narrow band filter, Birefringent crystals, Tunable filter.			18. Distribution Statement		
19. Security Classif. (of this report) Unclassified		20. Security Classif. (of this page)		21. No. of Pages 69	22. Price*

*For sale by the Clearinghouse for Federal Scientific and Technical Information, Springfield, Virginia 22151.

Figure 2. Technical Report Standard Title Page

TABLE OF CONTENTS

SECTION		PAGE
I.	INTRODUCTION	1
II.	DESIGN	5
	A. Optical	5
	B. Mounting Considerations	8
III.	CONSTRUCTION	10
	A. Filter System	10
	B. Calcite Crystals	17
IV.	PERFORMANCES	22
	A. Transmission	22
	B. Computer Control	24
	C. Thermal Properties	26
	D. Optical Quality	28
	E. Angular Characteristics	29
V.	CONCLUSIONS	31
	REFERENCES	34

I. INTRODUCTION

The purpose of this project was to construct a universal tunable birefringent filter and to document its construction features. In view of the documentation desires, major aspects in the filter design have been published in Solar Physics and Applied Optics. This report consists of three major parts - design, construction methods, and performance, with an introduction and conclusion. The introduction is a general view of the features of the filter as a whole while the conclusion contains directions for future research using this design as a base.

Previous to the Lockheed Alternate Partial Polarizer Universal Filter (LAPPU), one other universal birefringent design has been built by the Zeiss Corporation. Our filter differs in several significant ways from the Zeiss design. First, the fundamental requirement for a tuneable filter is achromatic half and quarter waveplates. Zeiss, following the design of Jacques Beckers¹, built waveplates using two materials with opposite retardation change with wavelength. The LAPPU uses achromatic waveplates made of sheets stretched polyvinyl alcohol (PVA) oriented in such a manner as to achieve achromatic retardation. The plastic waveplates are considerably less sensitive to wavelength variation than the crystal waveplates. They are also considerably cheaper to fabricate. (They can be fabricated in large sizes. A 1 m diameter waveplate is not unreasonable.) The waveplate materials are described in "Improvement of Birefringent Filters, I-Reduction of Scatter in Polaroid Materials."² This article describes the fabrication techniques for both low scatter polarizer and waveplate material. The design of achromatic waveplates is described in "Improvement of Birefringent Filters, II-Achromatic Waveplates."³ This article describes the theory of

multi-element achromatic waveplates. "Improvements in Birefringent Filters, III. Errors in Wide field Elements,"⁴ discusses the effect of departures from perfection of the multi-element waveplates and their impact on wide field element transmission.

A second major difference between the Zeiss filter and the LAPPU is in the crystal element length ratios and use of partial polarizers. All previous Lyot-Öhmon type birefringent filters have used length ratios of the form $L, L/2, L/4, \dots, L/2^n$, with high ($10^{+3} - 10^4$) transmission to rejection polarizers. The LAPPU uses length ratios $L, L/2, L/3, L/6, L/9, L/18, \dots$. Between elements with 2:1 length ratios, a polarizer with 3% leakage is used. Previously, Giovanelli and Jefferies,⁵ and Beckers and Dunn⁶ have theoretically discussed the effect of partial polarizers. However, no successful filter with partial polarizers had been built. "The Effect of Partial Polaroids in Birefringent Filters."⁷ discusses how a single partial polarizer effects the design of a birefringent filter. A detailed description of the design theory for general crystal lengths will be written for the fifth paper in the Improvement of Birefringent Filters series. The design section describes the rationale behind and the characteristics of the $L, L/2, L/3, L/6, L/9, L/18, L/27, L/54$ design used for LAPPU.

A third difference between the Zeiss and the LAPPU is the tuning method used. The Zeiss uses a single $l/4$ waveplate on each element which allows the element to be tuned by rotation of a polaroid. However, the rotating polaroid is the entrance polaroid for the next crystal element and as such must be at

45° to the crystal fast axis. Hence, all crystals after the first must rotate. In the LAPPU, an additional achromatic half waveplate is used with every other element with this system, it is necessary to only rotate half waveplates and polarizers.

In our opinion, there is significant advantage to not rotating crystals. Because of difficulties in fabrication, the field of view of elements is not exactly coincident and the axes of the elements. The axis also may not be co-linear. (When resolution of a fraction of an arc second is required from difference pairs very small image distortions become important.) We have examined the Zeiss universal owned by Dr. Zirin and have found significant field and axis effects. The Zeiss tunable HQ filter owned by Kitt Peak National Observatory shows similar effects. The effect of angular misalignment will be discussed in paper four of the Improvement series.

A fourth area of difference between the Zeiss and the LAPPU is in the area of tuning and thermal control. The Zeiss stores a set of polarizer and element positions for 20 lines in a diode matrix and tunes mechanically from these lines. The Sacramento Peak Zeiss has been modified to run directly from a Σ7 computer. The LAPPU also runs under control of a computer, in this case, a PDP11/10, which contains wavelength command programs. The tuning polarizers and half waveplates are run by eight independent stepping motors. There is no mechanical linkage between individual tuners. The design is completely modular, each element and its tuning control can be removed independent of the rest of the filter.

The thermal control of the Zeiss has a main thermal shroud controller and individual temperature controllers for each element. The stepping motors which are high heat output devices are mounted inside the thermal shroud which places large demands on the thermal control system. The LAPPU has temperature sensors mounted directly on each crystal. The computer can use this information to compensate the tuning for any temperature change. The filter is mounted in a substantial mass of aluminum and all the elements are in a common oil bath so that there is a considerable thermal inertia.

II. DESIGN

A. Optical

The design chosen for the filter is non-traditional in that successive elements are not a factor two shorter as in the standard Lyot design. Rather, successive pairs have lengths such that the sum of the lengths of the shorter pair is equal to the shorter element of the longer pair. Members of a pair have the traditional $\sqrt{2}$ to 1 length ratios. That is, the first four elements have lengths L , $L/2$, $L/3$, $L/6$. The advantage of these length ratios is that the polarizers between elements that differ by a factor of 2 may have a transmission to rejection ratio on the order of 10X. Since, for dichroic polarizers, the transmission in the pass direction decreases with the rejection to transmission ratio, the use of "poor" polarizers increases total transmission. For this filter there are four partial polarizers -- each with a transmission of .92. These replace polarizers of .84 transmission. As a result, the transmission is increased by a factor of $(.92/.84)^4 = 1.44$. An additional advantage of the design is that the need for a contrast element is eliminated, since the action of the partial polarizers is to internally self apodize the transmission.

The basic ideas of the design technique are discussed in "Partial Polaroids in Birefringent Filters."⁴ The fifth member of the Improvement of Birefringent Filters paper will describe the design techniques for general crystal lengths and general polarizers.

The only disadvantage of the partial polarizer design is that dichroic polarizers that are readily available have an insufficient polarization below 4500Å. However, with the design used here they can be readily replaced with

proper polarizers.-- which we hope to do in the not too distant future.

The filter actually constructed has crystal lengths of L , $L/2$, $L/3$, $L/6$, $L/9$, $L/18$, $L/27$, $L/54$, where L is 7.92861 cm. The total length of calcite is 17.912cm. Shown in Table 1 is the full width at half maximum (FWHM), the fraction of light inside FWHM, the fraction outside $2 \times$ FWHM, and $4 \times$ FWHM, the transmission of the filter at transmission maximum in polarized light, and epsilon, the partial polarizer factor. Epsilon is defined:

$$\epsilon = A_R / (A_P - A_R)$$

where A_R is the transmission amplitude in the rejection direction and A_P is the transmission amplitude in the pass direction.

The data for Table 1 was computed using LYTF5, a computer program for general combinations of retardation plates, rotators, waveplates, and partial polarizers. The input to the program was the actual configuration of the LAPPU, Beckers'⁸ analytic expression for calcite index difference and the measured performance of the actual polarizers used in the filter.

Shown in Figures 1 through 6 is the transmission and contribution function of the filter to the free spectral range for the six wavelengths of Table 1. The contribution function (shown dotted) is the fraction of the light outside the wavelength to half the free spectral range. It is defined as:

Table 1

λ	FWHM (\AA)	FRAC 1	FRAC 2	FRAC 4	TRANS	ϵ
6563	.132	.713	.083	.080	.457	.169
6103	.114	.715	.061	.058	.445	.187
5896	.104	.717	.070	.066	.424	.196
5374	.091	.767	.014	.009	.467	.422
5250	.091	.719	.031	.019	.467	.684
4861	.079	.684	.10	.062	.467	.892

$$c(\lambda) = 1 - \frac{\int_0^{\lambda} T(\lambda) d\lambda}{\lambda(\text{FSR}) \int_0^{\lambda} T(\lambda) d\lambda}$$

where $\lambda(\text{FSR})$ is the wavelength of half the free spectral range.

B. Mounting Considerations

The construction of wide field elements involves precise rotational alignment of the half waveplate with respect to the crystal halves. Paper three of the Improvement series discusses the required accuracies for the on-axis rays. Analysis of the error effects on the field of view of the filter shall be discussed in detail in paper four of the Improvement series. Here the field diameter changes will be illustrated. Shown in Figures 7 - 12 are computer simulated fringe patterns for a wide field element diffusely illuminated by a monochromatic source for half waveplates rotated by various amounts. The figures show the fringe patterns of the wide field elements, the patterns evolving from circular patterns, superimposed on a double hyperbolic pattern characteristic of narrow field elements. This representation is used because if the half waveplate is not perfect, faint hyperbolic fringes will be visible. Even if the waveplate is perfect on axis at some point off axis the hyperbolic fringes become visible.

From Figures 7 through 12 it is clear that an angular orientation of better than 0.1 radian ($.57^\circ$) is desirable and that the field of view is cut by a factor of two when the rotation error is .05 radians (2.87°).

The other important feature of the alignment of wide field elements is the relative tilt of the two crystals of the wide field element. Shown in

Figures 13, 14, 15 and 16 are fringe patterns for several tilts. The important result here is that elements can be properly aligned by comparison of the hyperbolic and circular fringes. For calcite, the relative displacement of the circular fringes is 10 times the displacement of the hyperbolic fringes, so that the construction technique is to center the circular fringes on the hyperbolic fringes by proper element tilt.

For a filter of 0.1\AA at 5000\AA , a resolution of 5×10^4 , the angular field corresponding to a shift of $.1\text{\AA}$ is about 5×10^{-3} radians, the angular alignment of the two halves of the wide field element must be at least a factor of 10 better than this. A more reasonable requirement is a factor of 50. Hence, the axial tilt alignment is on the order of 10^{-4} radians. Great care must be exercised to achieve such alignment. Keying techniques such as used by Zeiss or hexagonal prisms used by Halle are not sufficient to achieve such alignment.

Because of the alignment requirements, the design used here does not rotate any crystal elements. Rather, the filter consists of four modules consisting of quarter waveplate, crystal of the length L , half wave, crystal of length L , partial polarizer, crystal of length $L/2$, half wave, crystal of length $L/2$, and a final quarter wave. The elements are tuned by a separate assembly of a rotating polarizer and half waveplate.

III. CONSTRUCTION

A. Filter System

This section will illustrate the construction features of the LAPPU. Shown in Figure 17 are the eight wide field modules with temperature sensors attached. These modules are connected together in pairs and then mounted between the tuning assemblies. Figure 18 shows the crystal modules and tuning assemblies. Figure 19 shows the gear drives for the elements installed, and Figure 20 shows the complete optical-mechanical assembly of the filter. The entire housing shown in Figure 20 is filled with index matching fluid with an index of 1.52. The drive shafts to the rotating components are oil sealed. Seen on the top of the housing is the connector to the thermal sensors.

Shown in Figure 21 is the framework for mounting the eight stepping motors. Figure 22 shows the motors installed and wired. Figure 22 then represents the complete electro-optical assembly. The electro-optical assembly is electrically connected to motor controller drives, the thermal sensor multiplexer, and the zero position status logic. All of these are mounted on the interface chassis shown in Figure 23.

A flow chart for the interface chassis is shown in Figure 24. Fundamentally, the purpose of the chassis is to connect the PDPL1/10 control computer with the thermal sensors, stepping motors of the filter, and zero position sensors of the motors. The thermal sensors are connected to the computer through a A/D converter and a multiplex switch. A schematic of the input-output control lines is shown in Figure 25.

Shown in Table II is the detailed list of the optical train in the order light strikes them. Table III lists the sub-structure of the polarizers, partial polarizers, and waveplates. Table IV contains a list of filter material, cements, and oils. Shown in Figure 26 is an exploded view of a single module together with a schematic of its position in the filter. The components illustrated in the exploded view are numbered 34 through 54 of the optical train (Table II).

Table II

FILTER OPTICAL TRAIN

NAME	INDEX	RELATIVE ORIENTATION	NUMBER OF COMPONENTS	THICKNESS (cm)	COMMENT
1. Polarizer	1.52	0°	3/A	.386	Contacted to 2
2. Entrance window	1.52		1	.623	
3. Space	1.52			.0762	Oil filled
4. 1/2 wave	1.52	Rotates	5/B	.389	
5. Space	1.52			.0762	Oil filled
6. 1/4 wave	1.52	45°	6/C	.394	Contacted to 7
7. Element 1	Calcite	0°	1	.1461	Contacted to 8
8. Spacer	1.52		1	1.310	
9. Space	1.52			.0762	Oil filled
10. Partial polarizer	1.52	45°	5/D	.389	
11. Space	1.52			.0762	Oil filled
12. Spacer	1.52		1	1.166	Contacted to 13
13. Element 2	Calcite	90°	1	.292	Contacted to 14
14. 1/4 wave	1.52	45°	6/C	.394	
15. Space	1.52			.0762	Oil filled
16. Polarizer	1.52	Rotates	3/A	.386	
17. Space	1.52			.0762	Oil filled
18. 1/2 wave	1.52	Rotates	5/B	.389	
19. Space	1.52			.0762	Oil filled
20. 1/4 wave	1.52	45°	6/C	.394	Contacted to 21
21. 1/2 element 3	Calcite	0°	1	.221	Contacted to 22
22. 1/2 wave	1.52	45°	5/B	.389	Contacted to 23
23. 1/2 element 3	Calcite	90°	1	.221	Contacted to 24
24. Spacer	1.52		1	.627	
25. Space	1.52			.0762	Oil filled
26. Partial polarizer	1.52	45°	5/D	.389	
27. Space	1.52			.0762	Oil filled
28. Cover glass	1.52		1	.191	Contacted to 29
29. 1/2 element 4	Calcite	0°	1	.439	Contacted to 30
30. 1/2 wave	1.52	45°	5/B	.389	Contacted to 31
31. 1/2 element 4	Calcite	90°	1	.439	Contacted to 32
32. 1/4 wave	1.52	45°	6/C	.394	
33. Space	1.52			.0762	Oil filled

Table II (Continued)

NAME	INDEX	RELATIVE ORIENTATION	NUMBER OF COMPONENTS	THICKNESS (cm)	COMMENT
34. Polarizer	1.52	Rotates	3/A	.386	
35. Space	1.52			.0762	Oil filled
36. 1/2 wave	1.52	Rotates	5/B	.389	
37. Space	1.52			.0762	Oil filled
38. 1/4 wave	1.52	45°	6/C	.394	Contacted to 39
39. 1/2 element 5	Calcite	0°	1	.656	Contacted to 40
40. 1/2 wave	1.52	45°	5/B	.389	Contacted to 41
41. 1/2 element 5	Calcite	90°	1	.660	Contacted to 42
42. Cover glass	1.52		1	.191	
43. Space	1.52			.0762	Oil filled
44. Partial polarizer	1.52	45°	5/D	.389	
45. Space	1.52			.0762	Oil filled
46. Cover glass	1.52		1	.191	
47. 1/2 element 6	Calcite	0°	1	1.338	Contacted to 48
48. 1/2 waveplate	1.52	45°	5/B	.389	Contacted to 49
49. 1/2 element 6	Calcite	90°	1	1.299	Contacted to 50
50. 1/4 wave	1.52	45°	6/C	.394	
51. Space	1.52			.0762	Oil filled
52. Polarizer	1.52	Rotates	3/A	.386	
53. Space	1.52			.0762	Oil filled
54. 1/2 wave	1.52	Rotates	5/B	.389	
55. Space	1.52			.0762	Oil filled
56. 1/4 wave	1.52	45°	6/C	.394	Contacted to 57
57. 1/2 element 7	Calcite	0°	1	1.967	Contacted to 58
58. 1/2 wave	1.52	45°	5/B	.389	Contacted to 59
59. 1/2 element 7	Calcite	90°	1	2.001	Contacted to 60
60. Cover glass	1.52		1	.191	
61. Space	1.52			.0762	Oil filled
62. Partial polarizer	1.52	45°	5/D	.389	
63. Space	1.52			.0762	Oil filled
64. Cover glass	1.52		1	.191	Contacted to 65
65. 1/2 element 8A	Calcite	0°	1	2.417	Contacted to 66
66. 1/2 element 8B	Calcite	0°	1	1.833	Contacted to 67
67. 1/2 wave	1.52	45°	5/B	.389	Contacted to 68
68. 1/2 element 8C	Calcite	90°	1	2.284	Contacted to 69

Table II (continued)

NAME	INDEX	RELATIVE ORIENTATION	NUMBER OF COMPONENTS	THICKNESS (cm)	COMMENT
69. 1/2 element 8D	Calcite	90°	1	1.697	Contacted to 70
70. 1/4 wave	1.52	45°	6/C	.389	
71. Space	1.52			.0762	Oil filled
72. 1/2 wave	1.52	Rotates	5/B	.389	
73. Space	1.52			.0762	Oil filled
74. Exit window	1.52		1	.635	

Table III

COMPONENTS

	INDEX	ORIENTATION	PART NO.	THICKNESS (cm)	COMMENT
<u>Component A</u>					
<u>Polarizer</u>					
Glass plate	1.52		1	.191	Cemented to 2
HN-38 plastic	1.49	0°	2	.003	Cemented to 3
Glass plate	1.52		3	.191	
<u>Component B</u>					
<u>1/2 λ waveplate</u>					
Glass plate	1.52		1	.191	Cemented to 2
λ/2 sheet	1.49	0°	2	.002	Cemented to 3
λ/2 sheet	1.49	60°	3	.002	Cemented to 4
λ/2 sheet	1.49	0°	4	.002	Cemented to 5
Glass plate	1.52		5	.191	
<u>Component C</u>					
<u>1/4 wave plate</u>					
Glass plate	1.52		1	.191	Cemented to 2
λ/2 sheet	1.49	0°	2	.002	Cemented to 3
λ/4 sheet	1.49	60°	3	.002	Cemented to 4
λ/4 sheet	1.49	105°	4	.002	Cemented to 5
λ/2 sheet	1.49	45°	5	.002	Cemented to 6
Glass plate	1.52		6	.191	
<u>Component D</u>					
<u>Partial Polarizer</u>					
Glass plate	1.52		1	.191	Cemented to 2
HN-55	1.49	0°	2	.002	Cemented to 3
HN-55	1.49	0°	3	.002	Cemented to 4
λ sheet	1.49	90°	4	.002	Cemented to 5
Glass plate	1.52		5	.191	

Table IV

NOTES FOR FILTER OPTICAL TRAIN AND COMPONENTS:

1. Optical elements are contacted with Cargile type HV immersion oil.
Index = 1.515, viscosity = 46,500 cs.
2. The filter is oil filled with Cargile type A immersion oil.
Index = 1.515, viscosity = 150 cs.
3. The polaroid materials HN-38, HN-55, $\lambda/4$ sheet, $\lambda/2$ sheet and λ sheet have been cleared using techniques described in Improvement in Birefringent Filters I.
4. The polaroid materials are cemented with Kodak HF-4.

B. Calcite Crystals

Pertinent details of our method used to produce calcite elements with scatter-free polish, $1/8$ wave flatness, and minimum edge turn-down will be described. It should be recognized that our polishing methods, although successful for our universal filter, are not necessarily superior to that used by experienced commercial optical craftsmen. Recent commercial calcite elements which we have tested are generally equal in quality to ours and in some cases slightly superior. The processes used to produce such crystals is necessarily proprietary to commercial makers, and so by describing our methods we can perhaps provide information not presently available in the literature.

In any birefringent filter design, whether it be the earlier Lyot-Ohman or the partial-Polaroid design, all calcite elements must be worked to final very precise thickness ratios. This means that a deep scratch in final polishing can be disastrous. Calcite has the disposition of not just scratching, but fracturing, sometimes in excess of a millimeter deep. For this reason, our method had to be one which minimized this danger.

We believe that deep scratching is produced by calcite particles from rough unfinished outer edges. For this reason we prepared elements for polish by first grinding them on an Aluminum Oxide wheel to smooth cylinders and then fine grinding the sharp edges of the circular aperture to produce a smooth chamfer well below expected polishing depth.

For our thickest elements, the calcite crystals were not large enough or sufficiently homogeneous to afford the luxury of polishing and then later diaphraming or grinding to smaller aperture to eliminate bad filtering by edge turn-down. We found it necessary to find a polishing technique which produced minimum edge turn-down to preserve our final filter aperture of 33 mm.

In essence our method was one in final polishing of working crystals with concave surfaces and slowly decreasing the surface curvature, starting with a lap properly convex, several fringes, and finishing with a lap almost flat.

The convex lap will accelerate early polish of the calcite, centrally supported in its holder. It was noted that polishing in the concave to flat direction produced negligible edge turn on our calcite and pronounced edge-turn at the hole-edge in the holder. We found that if by chance it was necessary to polish in the direction from convex to flat, that this produced the reciprocal condition of pronounced edge-turn on the calcite with negligible edge-turn on the holder-hole. This may possibly be a well documented technique but we feel it is worth describing our experience.

For polishing we found "Linde A" recommended by R. Dunn to be the most satisfactory of all tested. Our polishing laps were made from 80 percent Burgundy Pitch and 20 percent Beeswax. They were 15 cm in diameter with facets 10 mm square. Our work was supported in white marble holders 7.6 cm in diameter with a supporting hole .25 mm oversize. The

holder and calcite element were pressed to a glass flat covered with a thin layer of silicone grease. Burgundy pitch was flowed into the .25 mm space at an oven temperature of 190°C . It is absolutely essential to avoid "thermal shock" to the calcite by raising oven temperature slowly, and then cooling the work completely to room temperature before sliding the work off the supporting glass plate.

After polishing, to remove the calcite from the holder, the work is again pressed with silicone grease to glass, and slowly heated to 175°C . At this point heavy insulated pot holders must be used to avoid any "thermal shock" to the calcite in extracting it from the holder. At such elevated temperature, inadvertently touching the calcite with the exposed hand will fracture it.

There may be supporting materials superior to pitch available commercially which would eliminate this dangerous temperature excursion in mounting, but in our experience we did not find any. Beeswax, although lower temperature melting, did not support the work properly.

For thinner elements to provide increased support we used silicone grease to add thicker clear glass cylinders to the crystal. For all elements thinner than the holder, this was done to permit safe excess pitch removal and allow clear viewing of hyperbolic fringes through the calcite during the polishing process.

With the method briefly described, we produced flat, scratch-free, well polished, parallel surfaces with negligible edge-turn. For most of the elements this was sufficient. However, for the thickest elements it was necessary to do some local figuring to compensate for minor calcite inhomogeneities. Local figuring was easier and more successful when done with the element still supported in its marble holder. We found that honeycomb beeswax laps supported on small flat tools dipped in a thin paste of "Linde A" provided scratch-free means of figuring small areas with good control. Great care must be taken not to exceed the corrective figuring required, and you must allow local heating produced in polishing to completely stabilize when assessing the progress of corrective polish.

Through the entire polishing operation besides monitoring the flatness of the surface figure, we also observed parallelism by watching the hyperbolic fringes produced between polaroids in monochromatic light (in our case, a Helium source). Especially in doing local figuring, it is important to determine unambiguously whether an area is thick or thin. This was best done by warming the spot with a finger and observing the change in the hyperbolic fringes. Increasing temperature will move the fringes in a direction corresponding to a thinner element. This, of course, is because the difference in calcite indices decreases and the element decreases in length with temperature increase (it increases in diameter though).

A final precaution in handling, cleaning, and assembling or disassembling finished calcite elements. The surfaces are extremely vulnerable

to abrasion, and will scratch or pit with even the most cautious treatment. Great care must be taken to omit any foreign particles in assembly with other surfaces. . Such particles can do great damage especialy in later dis-assembly, sliding elements apart.

IV. PERFORMANCES

A. Transmission

The theoretical transmission of the LAPPU using the measured value of polarizer transmission was presented in design section. These results are shown in Table I. Not included in the calculation was the fresnel reflection loss at each calcite to oil interface. There are 32 such interfaces, each with a loss factor of .001. The transmission reduction from this effect is .968. In addition the filter can lose transmission due to scatter, index mismatches at plastic and glass interfaces, and several types of misalignment. So that the calcite index mismatch corrected transmission is a best case upper limit upon the filters' transmission.

The filters transmission has been carefully measured at λ 6328. At this wavelength the corrected theoretical transmission is .436. The measured transmission was .35. However, at the time of measurement the filter did not have A-R coated entrance and exit surfaces. To compensate for the lack of these coatings the measured transmission is increased by a fresnel factor of 1.091 for a corrected transmission of .38. The operational transmission of the system is thus 0.88 of the maximum theoretical estimate. The Zeiss Universal, by comparison, has a transmission of 0.07 at λ 6328 and a FWHM of 0.22.

The filter measurement was made by monitoring the filter's transmission of a collimated He-Ne laser beam while each tuning component was rotated to achieve maximum transmission. The rotation sequencing and the settings to optimized positions was done by program SPIN. The laser beam was sampled both in front of and behind the filter to remove laser intensity fluctuations. When the transmission of the filter was maximized, the filter was removed from

the beam. The ratio of the intensities with the filter in and out of the beam is the measured transmission factor.

Accurate transmission measurements are difficult to perform on our spectrograph which has a theoretical resolution of 0.02\AA at λ 6328. Precision measurements shall be carried out in Feb. 1976 at Kitt Peak using the 10 meter spectrograph. Measurements of the filter transmission which have been made at Lockheed that show a FWHM that is consistently larger by $.02\text{\AA}$ than predicted (see Table I). However, the experimental measurements are consistent with the combination of the theoretical FWHM and spectrograph resolution, shown in Figures 27, 28 and 29.

B. Computer Control

The filter's computer control currently operates by driving the polarizers and waveplates to a set of position angles corresponding to the desired wavelength. Tuning near a set wavelength is accomplished by rotating waveplates and polarizers to angles that are proportional to the crystal lengths. Because the position of the waveplates and polarizers interact, a simple calculation is done for each tuning element. Currently the filter can be driven to any set wavelength in the visible and tuned plus or minus sixteen angstroms with essentially the same line profile. At any wavelength temperature compensation is done by sensing the individual thermistors and tuning the elements using an assumed wavelength shift with temperature.

For manual checks each tuner can be cycled directly from the computer control console. The temperature of all the crystals can be printed on the teletype either once or every 10 seconds by a key command.

In addition to the wavelength setting and tuning programs, there are several programs that utilize one or more intensity monitors that can be read by the computer. The transmission measurement was carried out, for example, by program SPIN. SPIN takes the output of two photodiodes before and one after the filter and uses the relative intensity information to optimize the filter's transmission of a He-Ne laser beam. SPIN rotates each tuning element in succession through its tuning range. For each tuning component, the position of maximum transmission is stored and the tuner set to that position. It has been experimentally discovered that regardless of start position

four iteration of the SPIN process yields a stable maximum filter transmission.

The SPIN program has also been used as a subroutine in the thermal monitoring procedure. Here it has allowed determination of the temperature sensitivity of calcite.

C. Thermal Properties

Proper performance of a very narrow birefringent filter depends on accurate thermal control or compensation for thermal effects. Individual calcite elements drift in wavelength by approximately $.03\text{\AA}/\text{C}^\circ$ at 6000° . For a filter of 0.1\AA bandpass, it is desirable to control the temperature to 0.01\AA or 0.0333°C .

In the IAPPU direct temperature control to a few hundredths of a degree is not attempted. Rather the tuning capability of the filter is used to compensate for measured temperature changes. The requirement for stable operation then is that the response of the filter to the thermal inputs of the control mechanism are slow compared to the control rate.

In order to test the sensitivity of the filter to motor heating the motors were all turned on for 30 minutes. During the period of motor heating and for one hour thereafter the values of the resistance thermal sensor elements were printed out every 15 seconds. The sensors did not indicate a change of more than one count, a temperature change of $.005^\circ\text{C}$, until 35 minutes after turn motor off. The sensors reached a peak temperature 45 minutes after turn off. In normal operation motors are on only when the filter is changing wavelength. So that this test is a worst case situation.

In order to test the thermal control algorithm the filter was tuned to transmit a He-Ne laser beam and the transmitted intensity was recorded. Every $\frac{3}{4}$ minutes the filter optimization program was run. Shown as a solid line in Figure 30 is the filter transmission versus time. The crosses are the optimized transmitted intensity.

Based on the experiments it is not unreasonable to expect that the filter maintain a set wavelength to an accuracy of 0.01\AA for hours. The main source of wavelength drift is the temperature sensor electronics. We plan to include a small He-Ne laser and flip mirrors into the filter control loop. The laser system shall allow periodic recalibration of the thermal sensor system.

D. Optical Quality

The final test of optical quality is a high resolution picture. Unfortunately, this report is being written during the winter and sufficiently good seeing is not available. However, interferograms have been taken through the filter. Shown in Figure 31 are LUPI (Laser Unequal Path Interferometer) interferograms of the filter. The filtergrams were taken in λ 6328 light with the filter tuned to λ 6328. Substantially the same interferograms were obtained when the tuning components were rotated by 180° . The tuning components, polaroids and a half wave plate, have been the same filtering effect at angles of alpha and alpha $+180^\circ$.

In our opinion the invariance of the interferograms to rotation of the eight tuning components by 180° indicated that the wave front distortions are coming from the fixed filter components.

At present we do not know where the wavefront distortions arise. However, at some time in the future we shall dismantle the filter and check each component critically on the LUPI. In any case, the interferograms seem to indicate that the filter introduces a curvature of less than 2 waves plus a cylinder of 2 waves. When the filter is used in an $f/30$ beam, 15 cm from the focal plane the focus changes introduced by the wavefront distortions are less than one tenth the diffraction limited depth of field.

E. Angular Characteristics

As discussed in the design section, the angular characteristics are sensitive to the alignment of the wide field elements. Shown in Figure 32 is a photograph of the angular characteristic of a typical wide field element. For the figure the achromatic waveplate was replaced with a normal halfwave so that the faint hyperbolic fringes could be photographed. Actual filter wide field elements are aligned better than shown in Figure 32.

In assembly, the circular patterns of all the wide field elements were made coaxial. The only loss in field of view arose because the final element's halves are not exactly equal giving rise to an elliptical field of view. The principal axes of the ellipse differ by less than five percent. So that the field of view is essentially the theoretical field.

For a wide field filter in a collimated beam, the shift in wavelength with angle is a quadratic function of angle. If the maximum allowed shift is $\pm \text{FWHM}/10$, then at 6500\AA and 4500\AA , the field of view of the filter is 2.6° and 2.0° , respectively. However, for this to be the useable field of view, the filter must be in front of the objective. When the filter is not in front of the objective, but in a collimated section, the field of view is reduced by the ratio of the diameter of the filter aperture to the telescope entrance. For a 35 mm aperture filter on a 305 mm diameter objective telescope, the fields of view at 6500\AA and 4500\AA are 0.30° and 0.22° respectively.

It is unrealistic, however, to expect to use a birefringent filter in a collimated beam because the optical quality is seldom sufficiently high. To minimize aberrations, a birefringent filter should be used as close as is practicable to a focal plane. To eliminate angular shifts with angular position, the beam through the filter must be telecentric. If a 10 percent increase in FWHM is tolerable at 6500Å and 4500Å, f/20 and f/25 respectively, telecentric beams are required. For a 3 percent allowed increase in FWHM at 6500Å and 4500Å, f/30 and f/36, respectively, beams are required. If the filter is near the focal plane, the field of view in a telecentric beam is the focal ratio times the ratio of filter to objective apertures. For a 35 mm filter and 305 mm objective telescope field of view is 0.31° in an f/20 telecentric beam.

V. CONCLUSIONS

The filter reported here can be improved upon in several ways. The first is in the performance of the polarizers which both lose a factor of two in light and also limit the wavelength range of the filter. A second possible improvement is in the area of increasing resolution. A third in increasing the free spectral range. Finally, great improvement would result from the installation of reliable electro-optic retardation plates.

The polarizers normally used in birefringent filters are sheet plastic polarizers made by Polaroid Corporation or German polarizers supplied by Zeiss and Halle. Typically, these have transmissions in the pass direction of .85 for high rejection polarizers. Both dielectric polarizers and crystal polarizers can be made with .98 or greater transmission. Unfortunately, both of these elements are cubical or worse in shape and hence add a great deal of length to an already long optical path. With some design effort, good wide band dielectric polarizers that operate at 60° to the optic axis could be available. Sixty degree polarizers would still require lengths of optical path equal to half the clear aperture.

Perhaps a solution to the polarizer problem can be obtained by brute force. That is, the polarizers could be exchanged depending on operating wavelength. With the polarizers that are not required to rotate for tuning, the concept of polarizer exchange becomes fairly reasonable, especially with the partial polarizer design which allows half the polarizers to have low rejection ratios. A set of three polarizers should allow good filter performance from 3,500 to 14,000Å. And, of course, some research into sheet polarizers may mean only two sets are required.

The filter developed here has a 8 cm final element. For a factor of 2 decrease in bandwidth, it will require 16 cm in final element. Hopefully, we shall fabricate a 0.05Å element for this filter in the coming year. However, another factor of 2 will be very hard. Also, recall that the filter now has 18 cm of calcite -- a factor of 2 makes this 36 cm, and 2 again, 72 cm, neglecting all the required waveplates and polarizers. One solution may be to double pass the longer elements. We have tried this semi-successfully for the two longest elements of a filter. The "semi" refers to the fact that the spectral performance was achieved on the spectrograph, but multiple images resulting from the double pass operation existed. Because of time requirements, extensive double pass experiments were not carried out.

Universal double pass filters will require the development of broad band polarizing beam splitters, and perhaps high quality corner reflectors. But to really extend the resolution of narrow band filters, it will be necessary to develop Michelson final elements. A resolution of 10^5 at 5000Å requires a path difference of 2.5 cm, for calcite which has index difference to index ratio of 10 -- this means 25 cm of calcite. A wide field Michelson would require the aperture diameter plus 2.5 cm in length. A Michelson at fixed spacing is optically identical to a birefringent element. In fact, the idea of a Michelson filter has its origin in the 1949 classic paper of Evans.⁹

The present filter has a free spectral range of 14Å at H α (6563) and .8Å at H β (4861). A state-of-the-art blocker can successfully isolate the solar lines. Currently, the best all-deposited dielectric filters have half widths

of 3\AA . It is unlikely that a factor of two narrowing will be achieved without significant effort. In any case, the desire to tune several Angstroms in the region of a line probably means that there is not much point in lowering the free spectral range of the filter. A quartz universal filter of nine elements could extend the free spectral range to nearly 4000\AA . Hopefully, the transmission would be 50% in polarized light which is competitive with the transmission of a 4\AA blocker.

Tuning of this filter is accomplished by mechanical rotation of polarizers and waveplates. It would be highly desirable to tune the filter electrically using electric waveplates. Extensive experiments were carried out with KDP plates. However, we were not able to fabricate reliable electrode structures for D.C. operation (less than 200 Hz). One experimental waveplate lasted two weeks at 3000 VDC before failure. There is some possibility that transparent electrodes could be cold sputtered on KDP or some other electro-optic crystal. Attempts to purchase electric waveplates has also failed. Currently we have an outstanding order for two electric waveplates with cold sputtered electrodes.

REFERENCES

1. J.M. Beckers; Appl. Opt. 10, 973 (1971).
2. A.M. Title; Solar Physics 33, 521 (1973).
3. A.M. Title; Appl. Opt. 14, 229 (1975).
4. A.M. Title; Appl. Opt. 14, 445 (1975).
5. R.G. Giovanelli and J.T. Jefferies; Austr. J. Phys. 7, 254 (1954).
6. J.M. Beckers and R.B. Dunn; AFCRL Instr. paper 75, 31.
7. A.M. Title; Solar Physics 38, 523 (1974).
8. J.M. Beckers and R.B. Dunn; AFCRL Instr. paper 75, 4.
9. J.E. Evans; JOSA 39, 142 (1949).

FIGURE CAPTIONS

- Figures 1-6 Plots of Log transmission (solid) and contribution (dot) versus wavelength from transmission peak to free spectral range for:
- 1) $\lambda 6563$
 - 2) $\lambda 6103$
 - 3) $\lambda 5896$
 - 4) $\lambda 5374$
 - 5) $\lambda 5250$
 - 6) $\lambda 4861$
- Figures 7-12 Simulated fringe locations for a wide field element illuminated by diffuse monochromatic light. Both wide field fringes and narrow fringes caused by an imperfect half wave are shown. Shown are effects of rotation of the half wave.
- 7) 0.0 radians
 - 8) 0.02 radians
 - 9) 0.045 radians
 - 10) 0.05 radians
 - 11) 0.055 radians
 - 12) 0.07 radians
- Figures 13-16 Simulated fringe locations of a wide field element with imperfect half wave for tilt of the elements with respect to each other by a fraction of the alignment requirement for the narrow field element.
- 13) Tilt fraction = 0.1
 - 14) 0.5
 - 15) 1.
 - 16) 9.
- Figure 17 Photograph of the eight calcite modules in brass containers with temperature sensor attached.
- Figure 18 Element modules mounted between tuning sections.

- Figure 19 Gear assemblies attached to tuning sections.
- Figure 20 Complete optical-mechanical assembly.
- Figure 21 Optical-mechanical with motor mounts.
- Figure 22 Complete universal filter.
- Figure 23 Filter computer interface chassis.
- Figure 24 Flow chart for filter computer interface.
- Figure 25 Connector schematic for interface.
- Figure 26 Exploded view of filter module optics
- Figure 27 Measured transmission profile at λ 5896.
- Figure 28 " " " λ 5324.
- Figure 29 " " " λ 4861.
- Figure 30 Filter transmission in A/D converter units versus time using thermal control algorithm. Crosses are optimized filter transmission. Crosses are displaced upward for visual convenience.
- Figure 31 LUPI interferograms
- Figure 32 Typical field of view of wide field element.

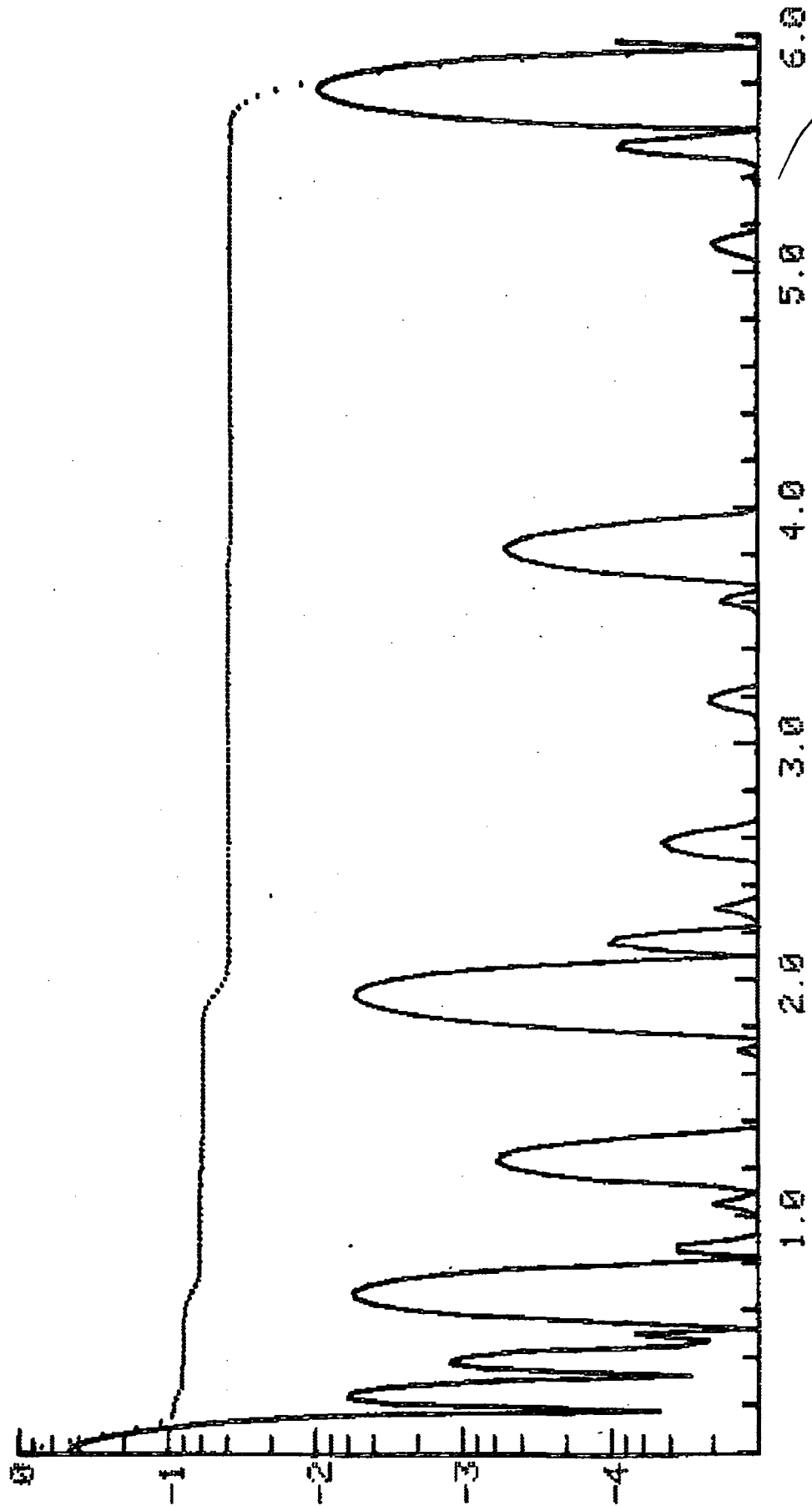


Figure 1 $\lambda 6563$ $\epsilon = 0.17$

6-17-68

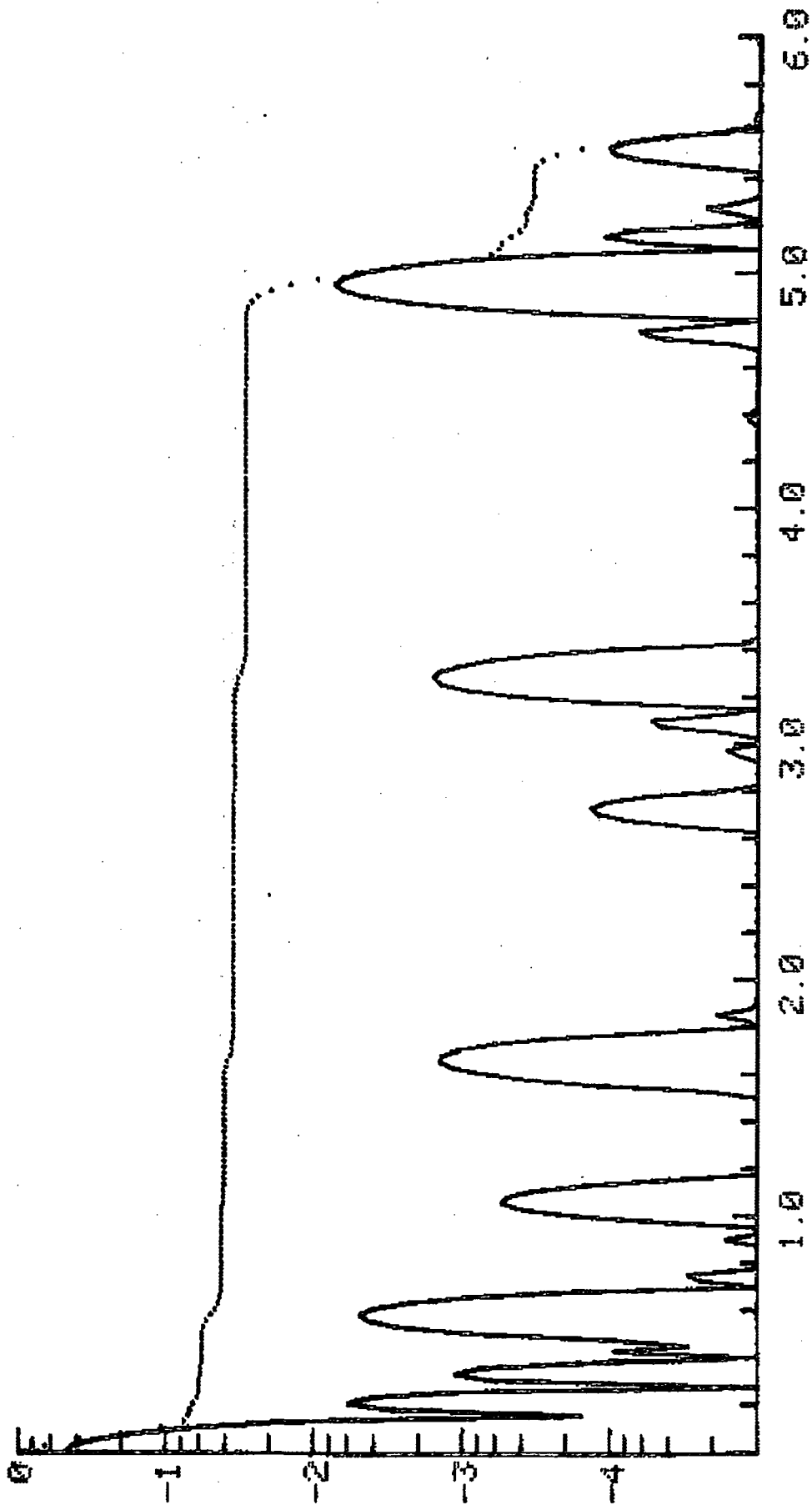


Figure 2 $\lambda 6103$ $\epsilon = .187$

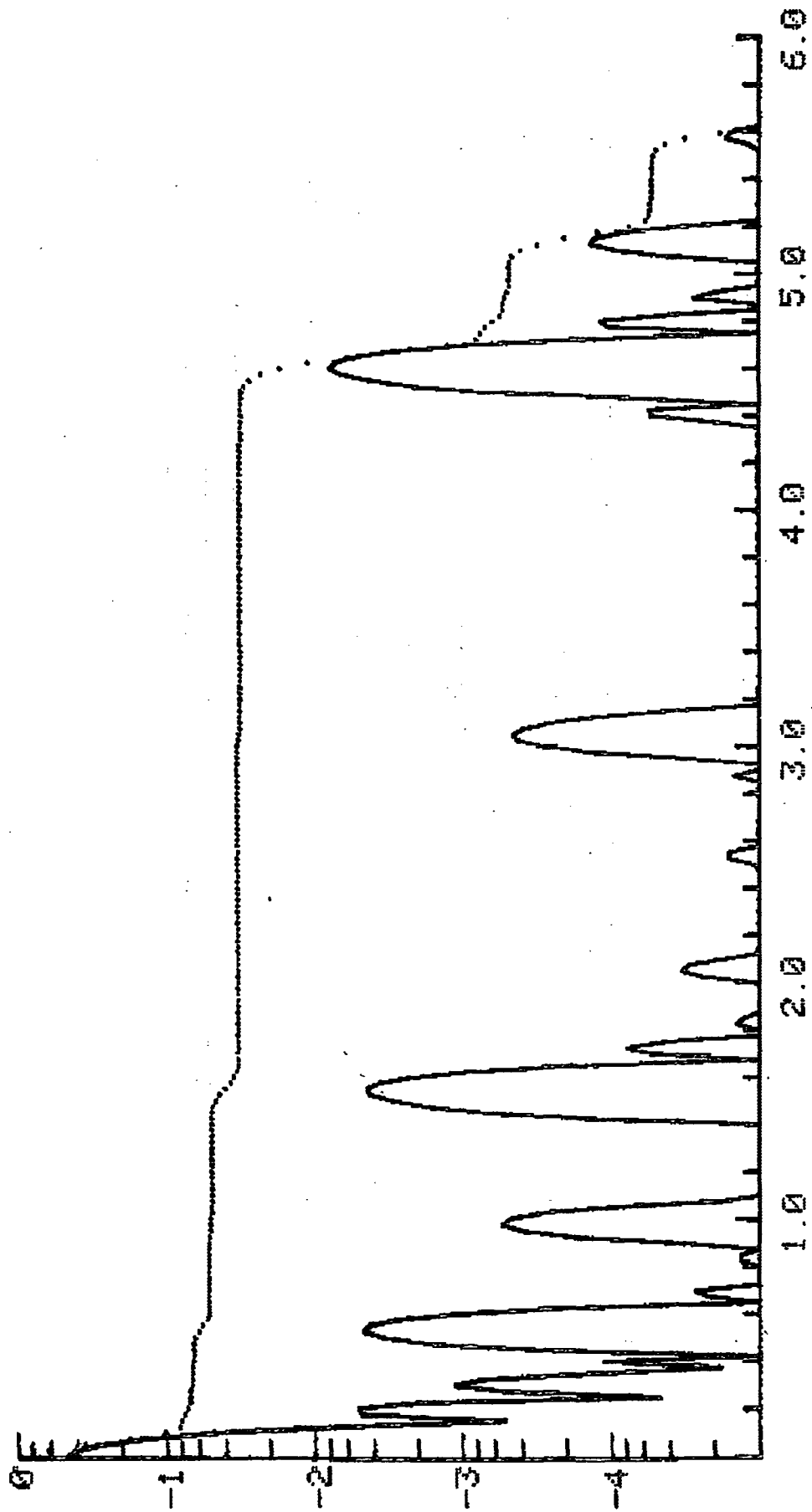


Figure 3 $\lambda 5896$ $\epsilon = .195$

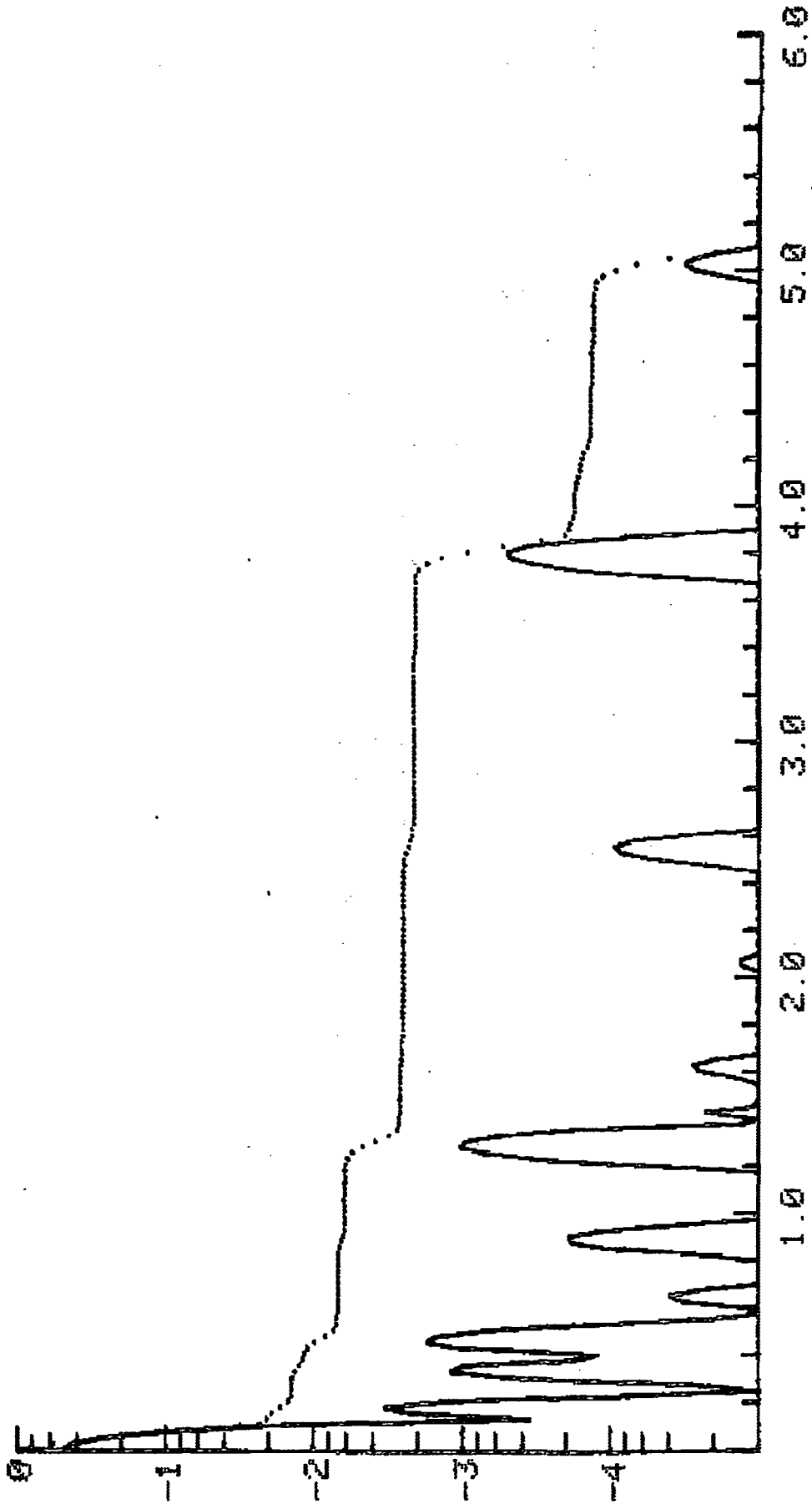


Figure 4 $\lambda 5374$ $e = .413$

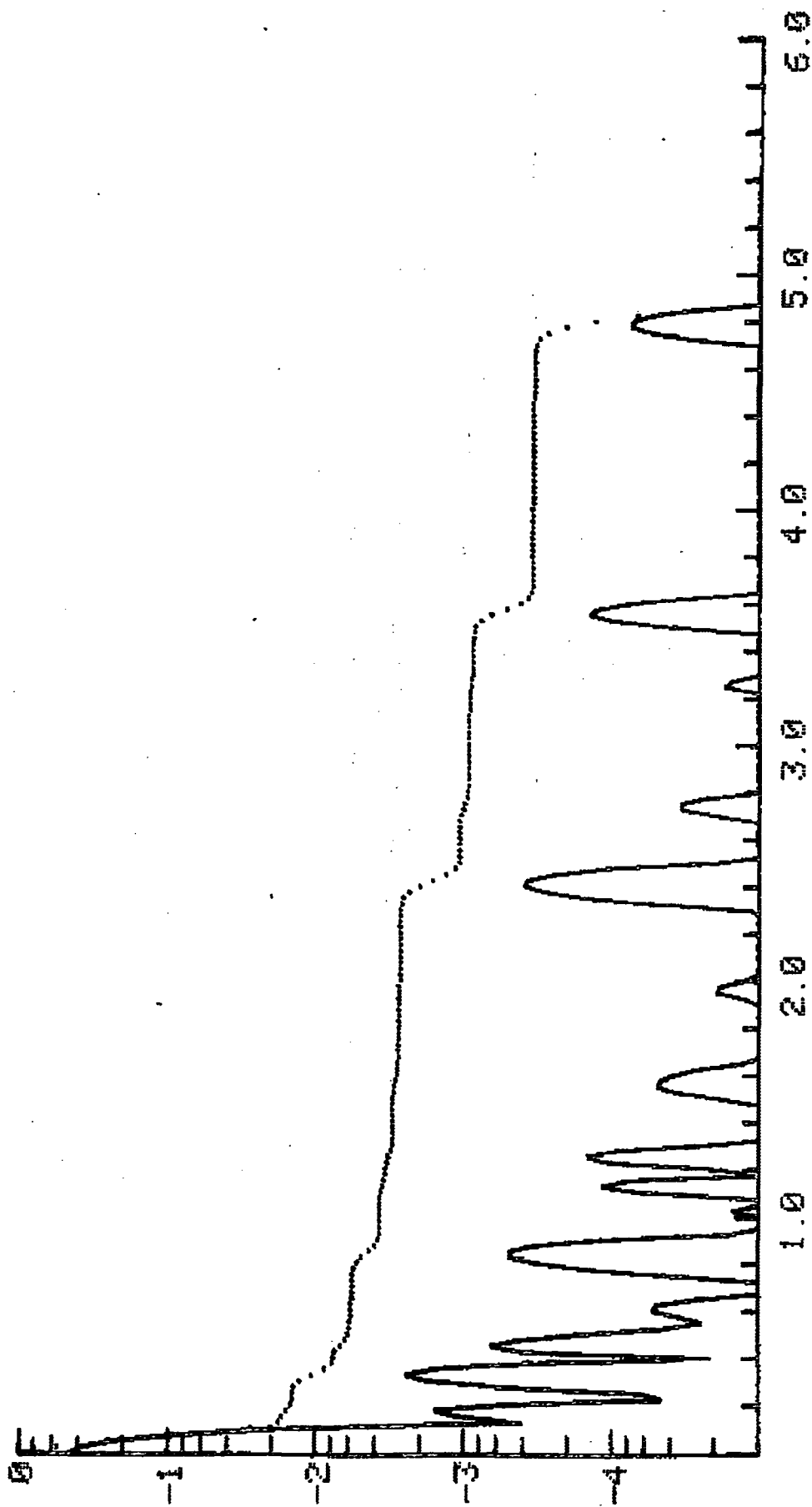


Figure 5 $\lambda 5250$ $\epsilon = .538$

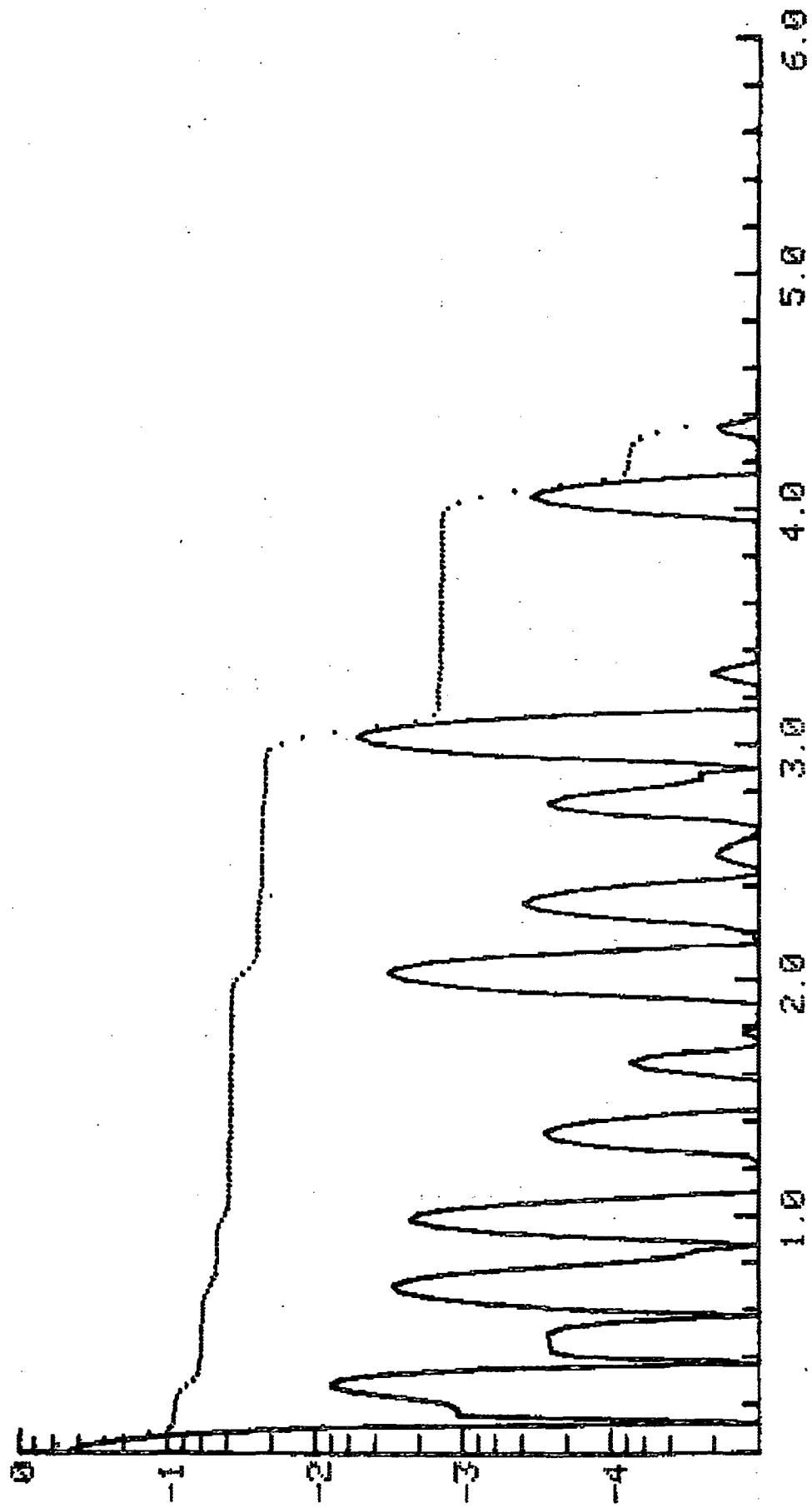


Figure 6 $\lambda 4681$ $\epsilon = .90$

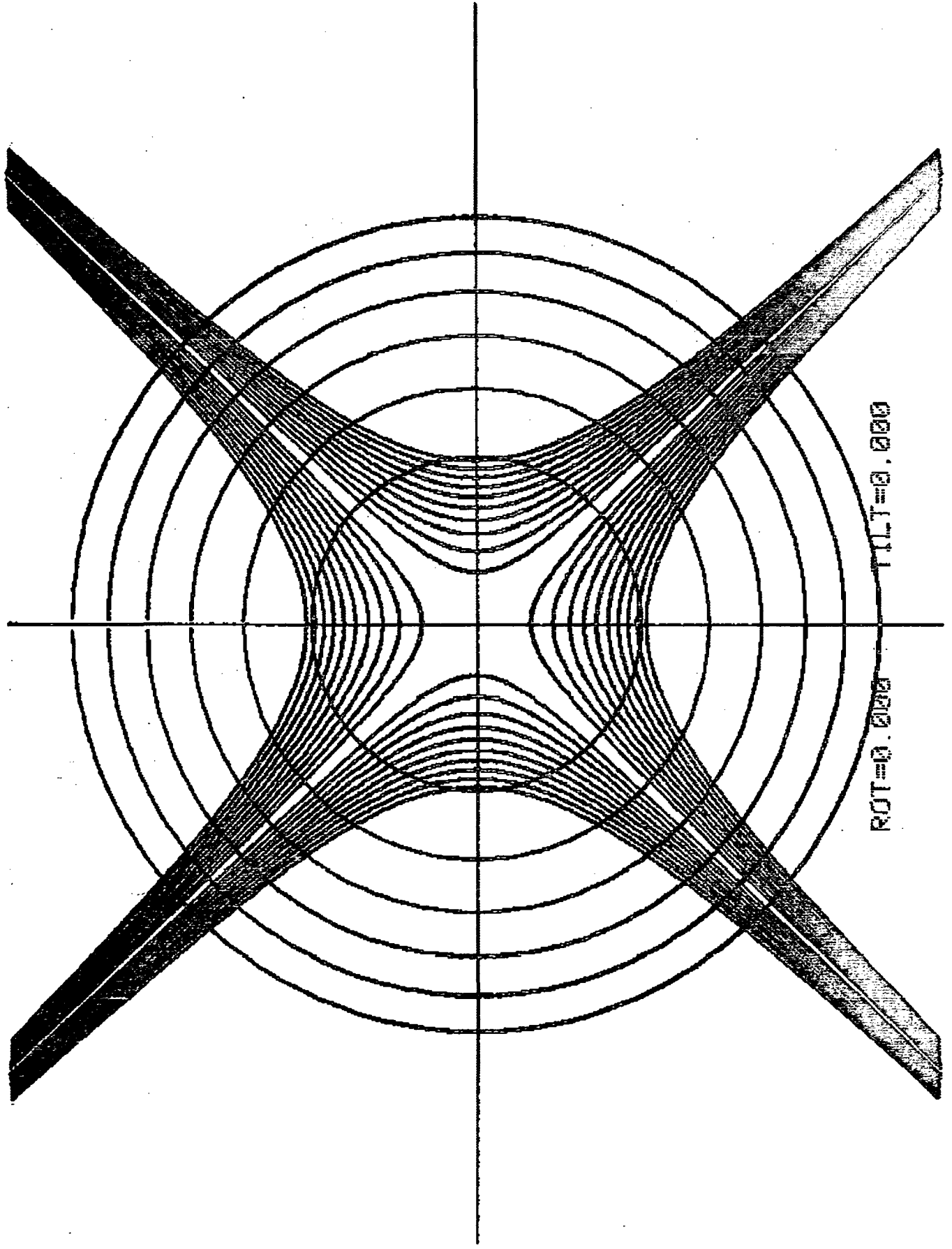


Figure 7

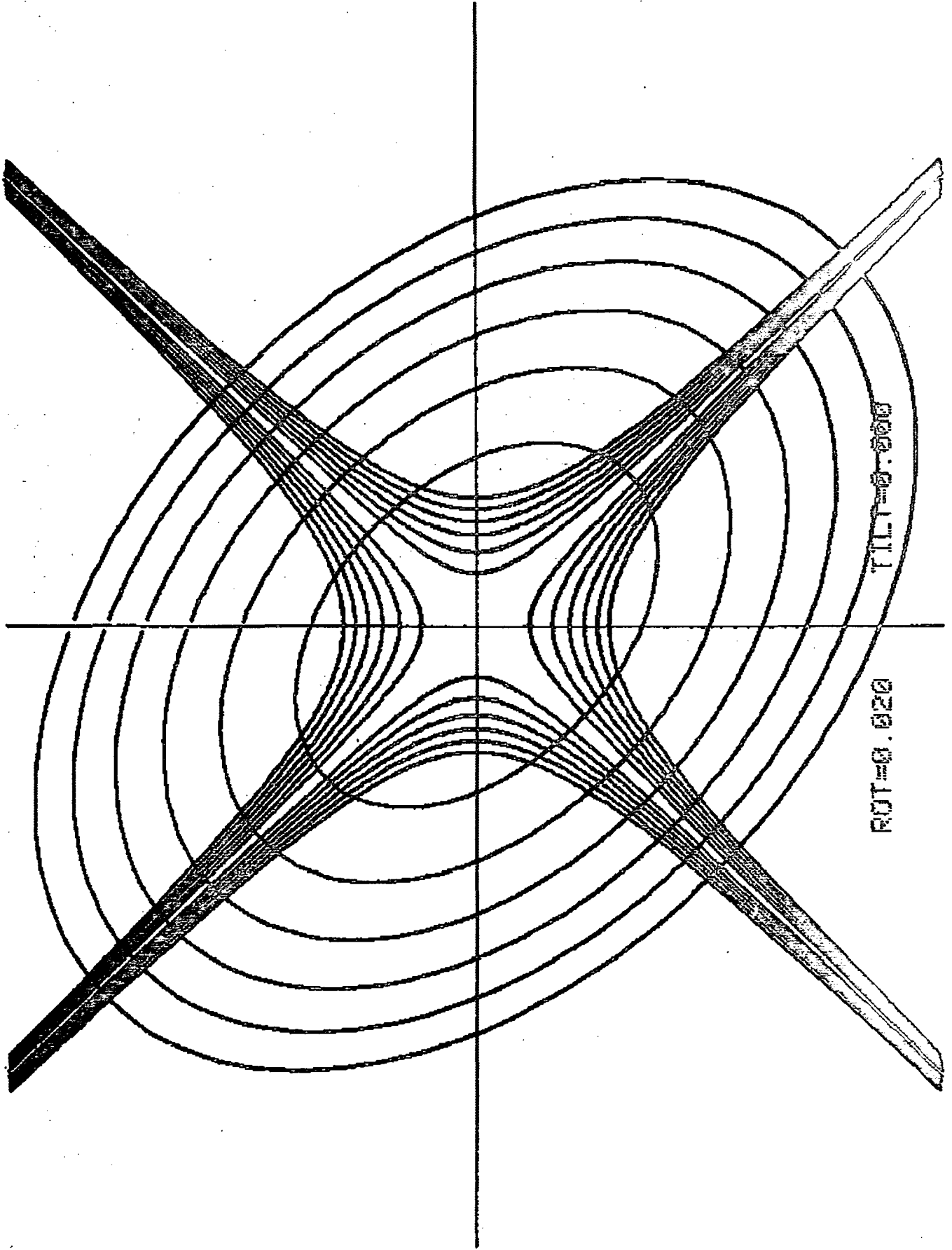
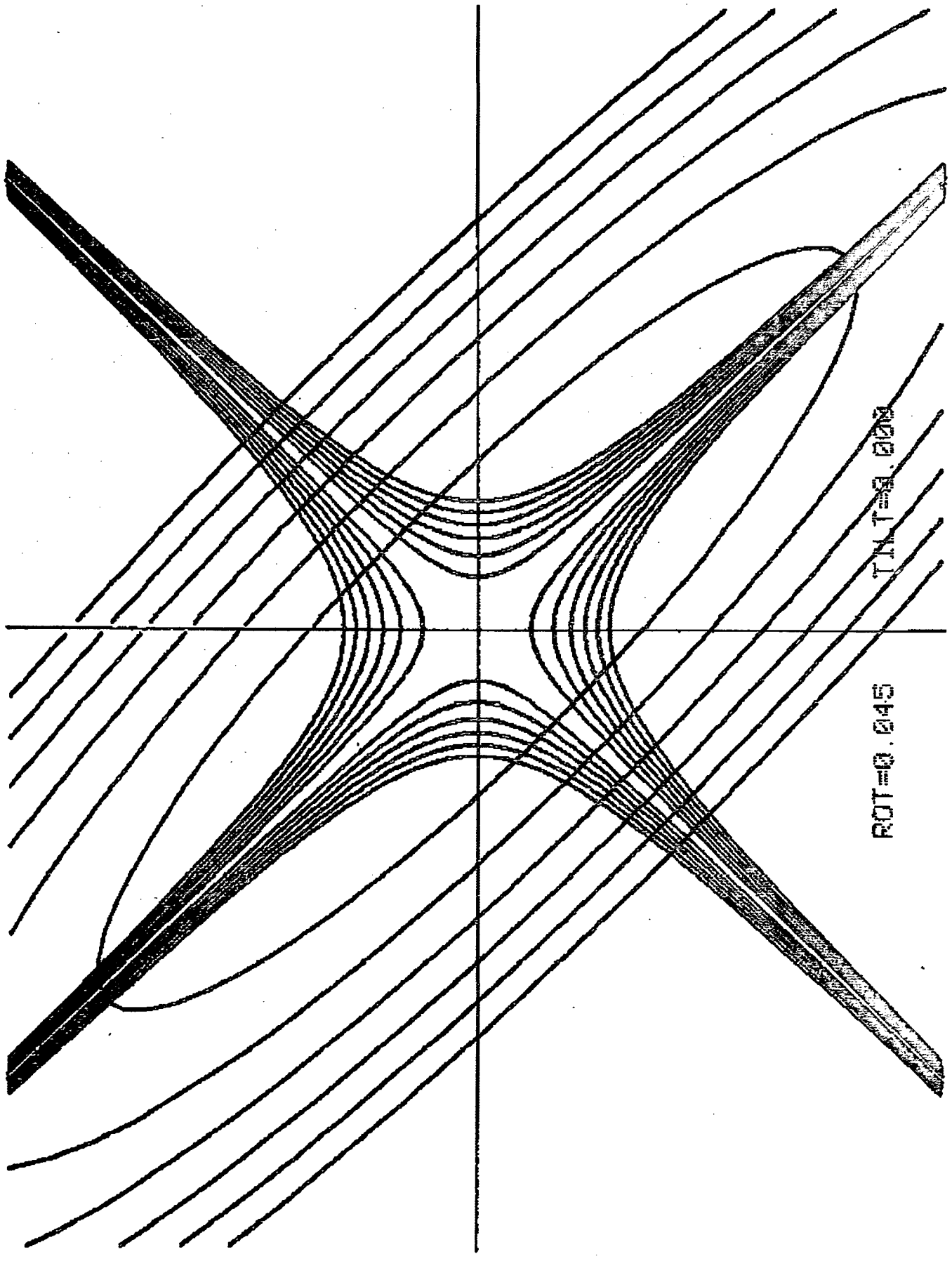


Figure 8



T.M.T=9.020

ROT=0.045

Figure 9

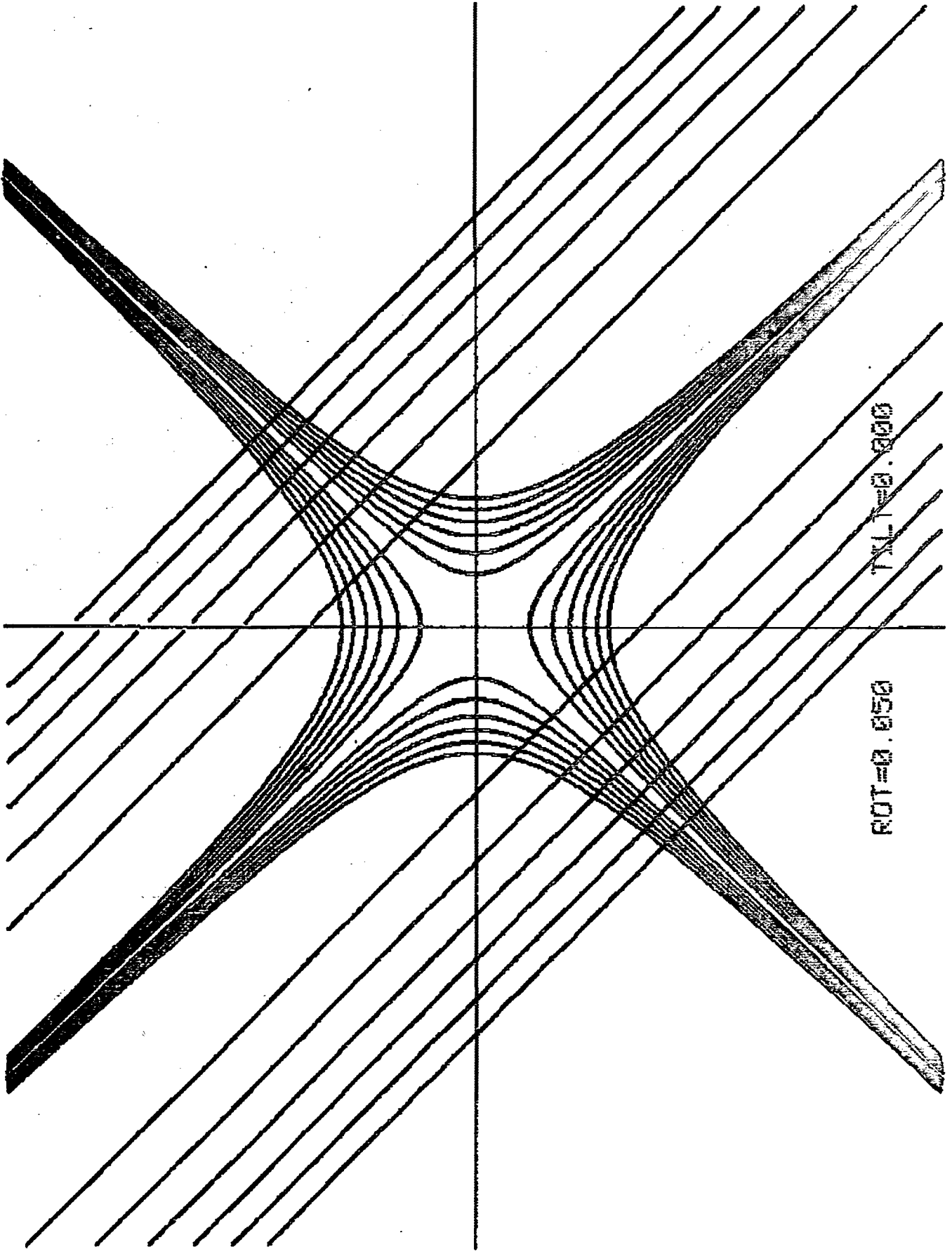


Figure 10

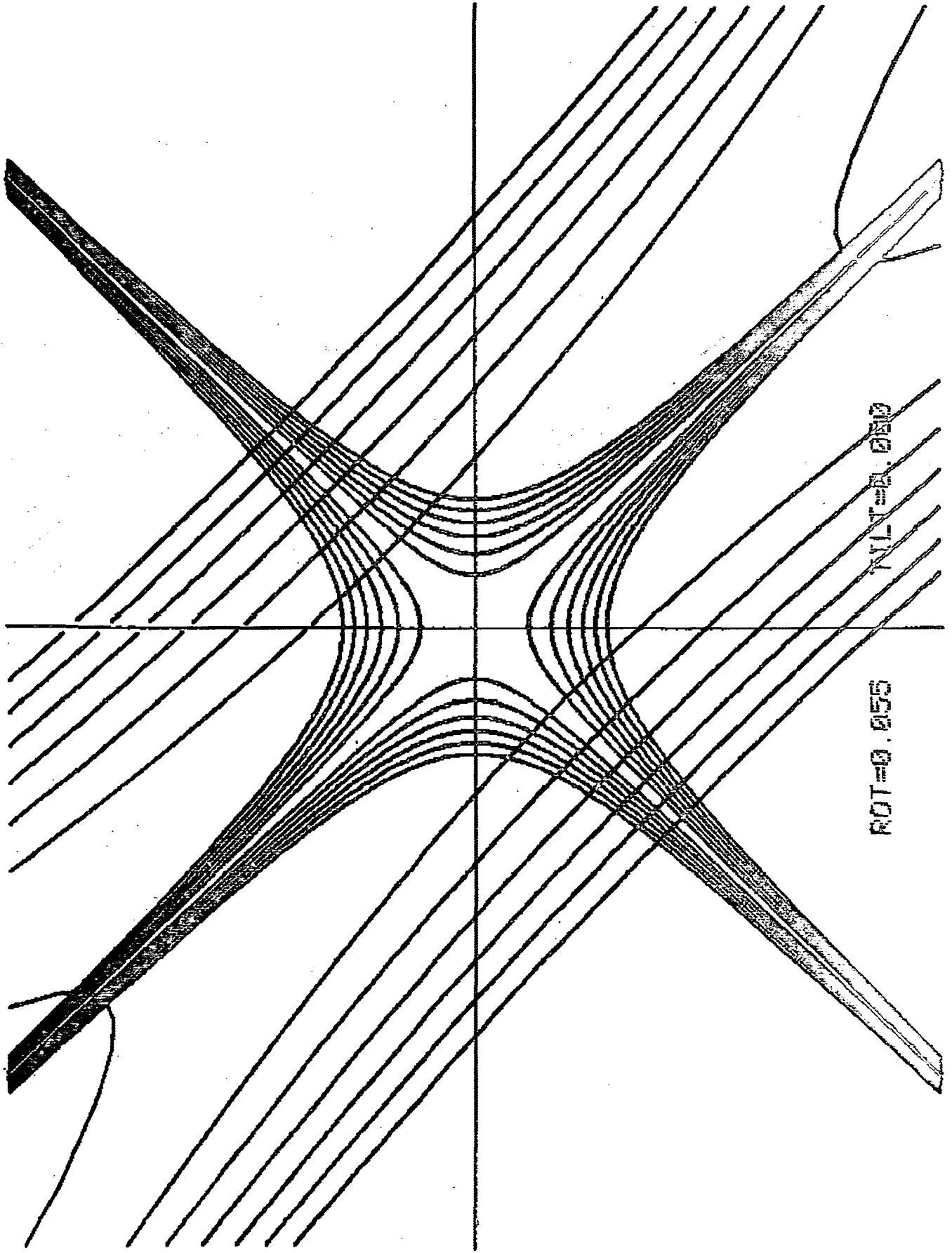


Figure 11

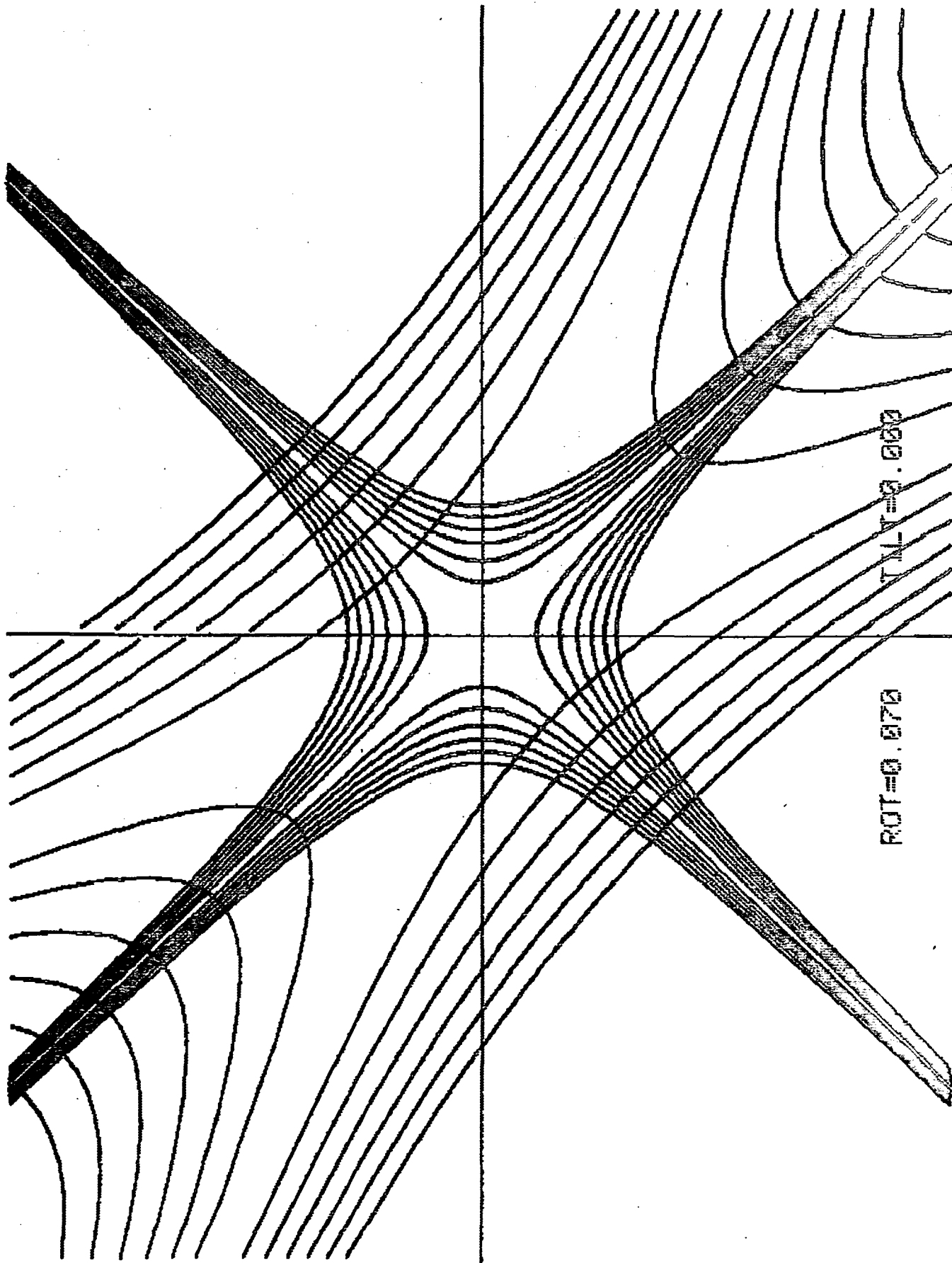


Figure 12

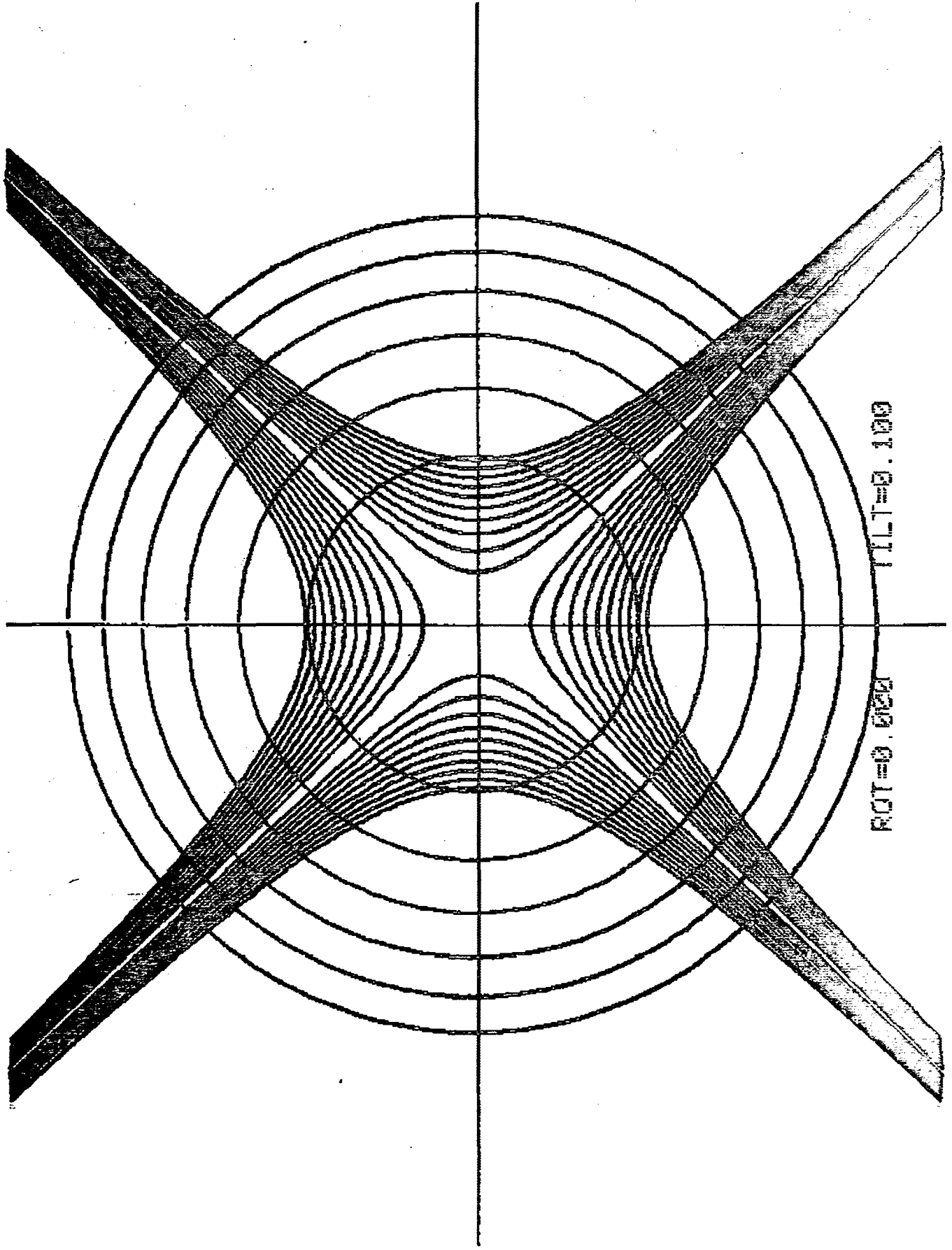


Figure 13

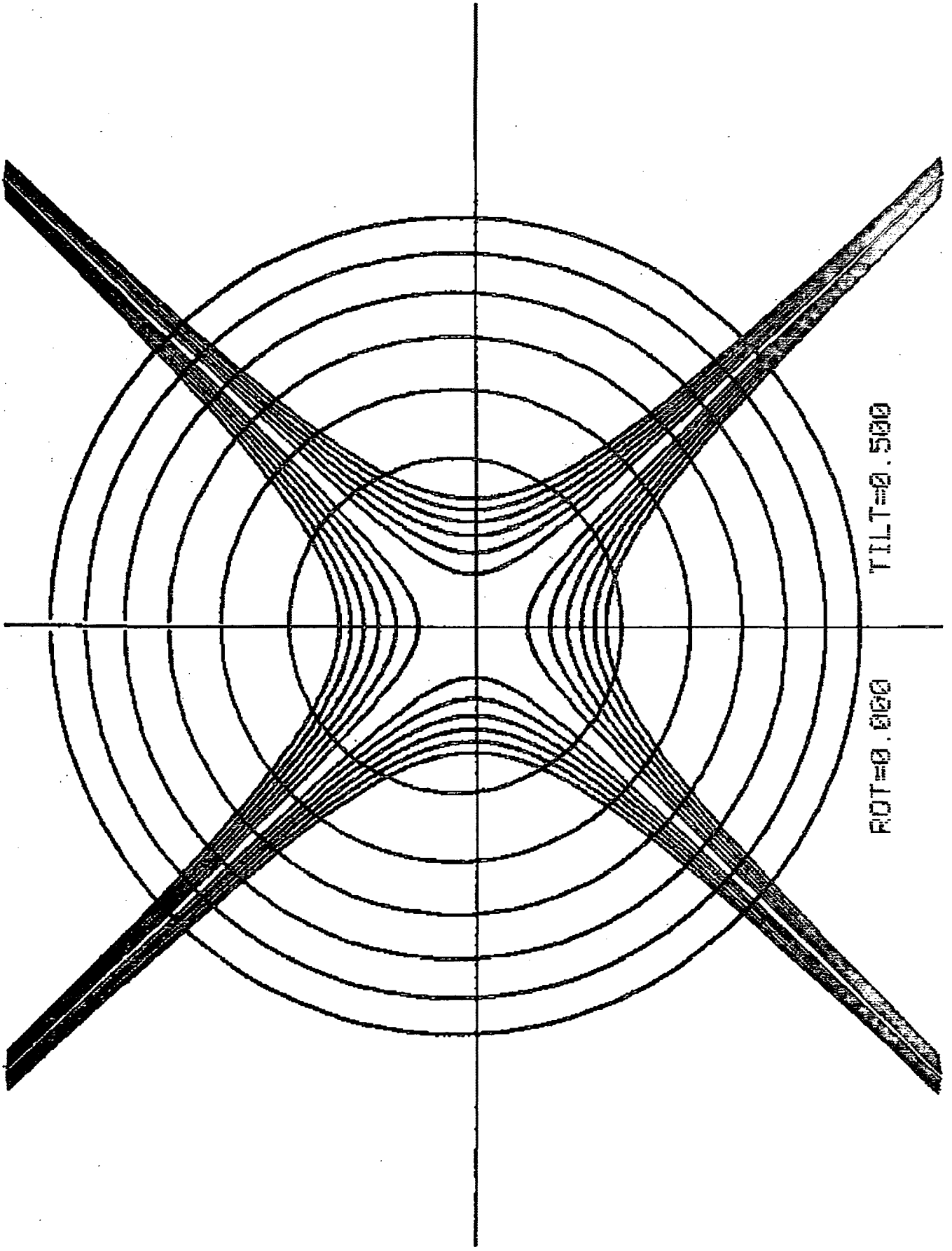


Figure 14

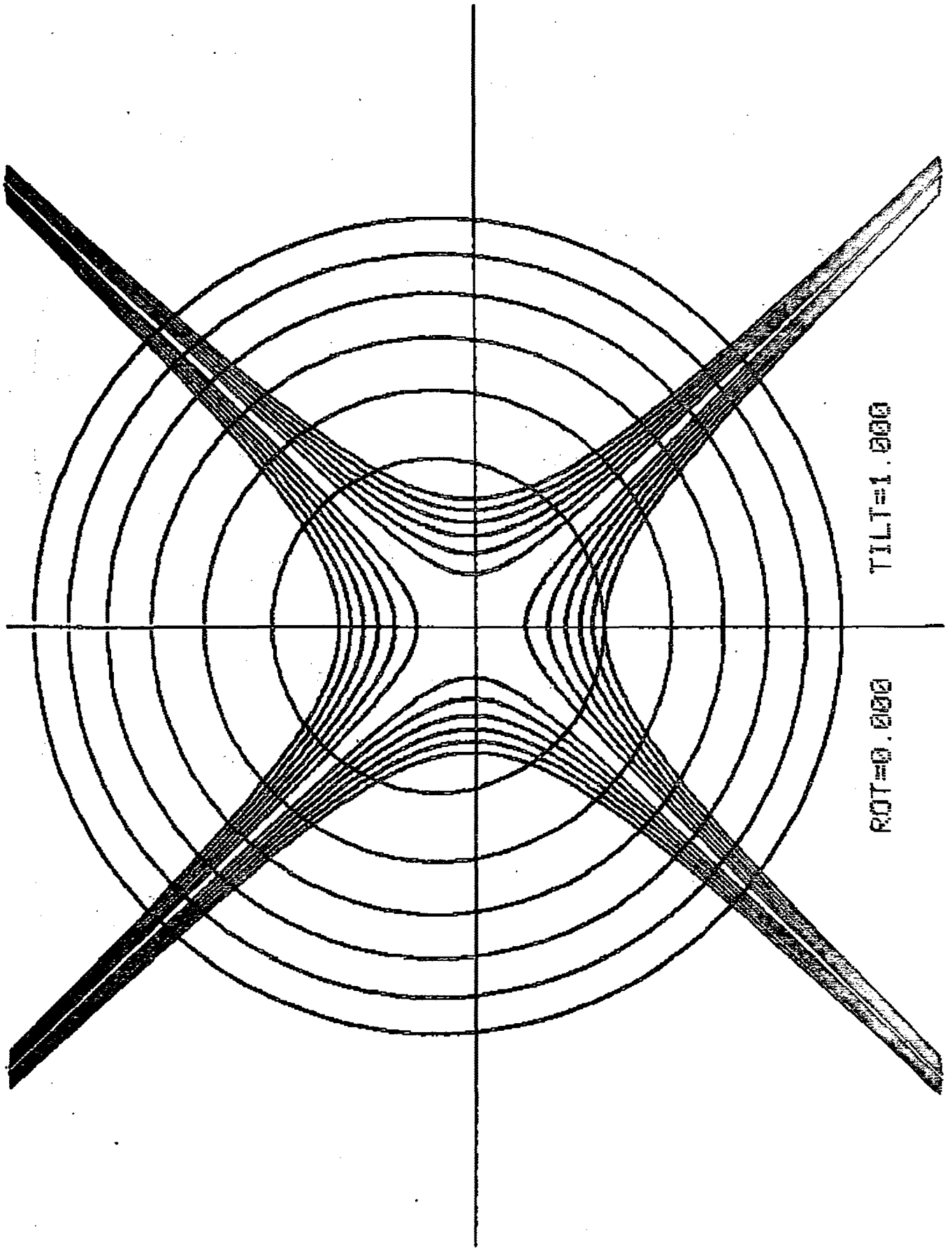


Figure 15

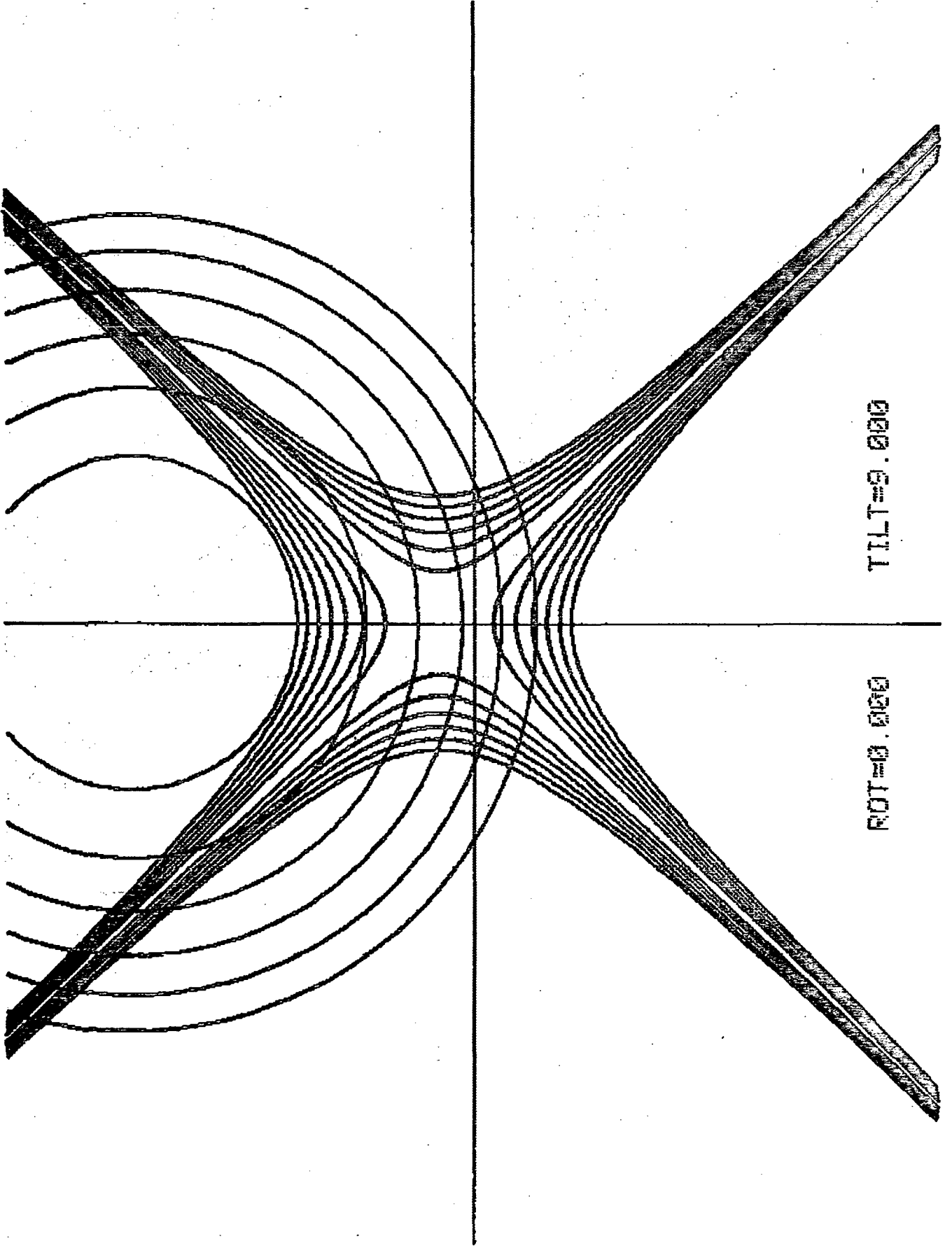


Figure 16

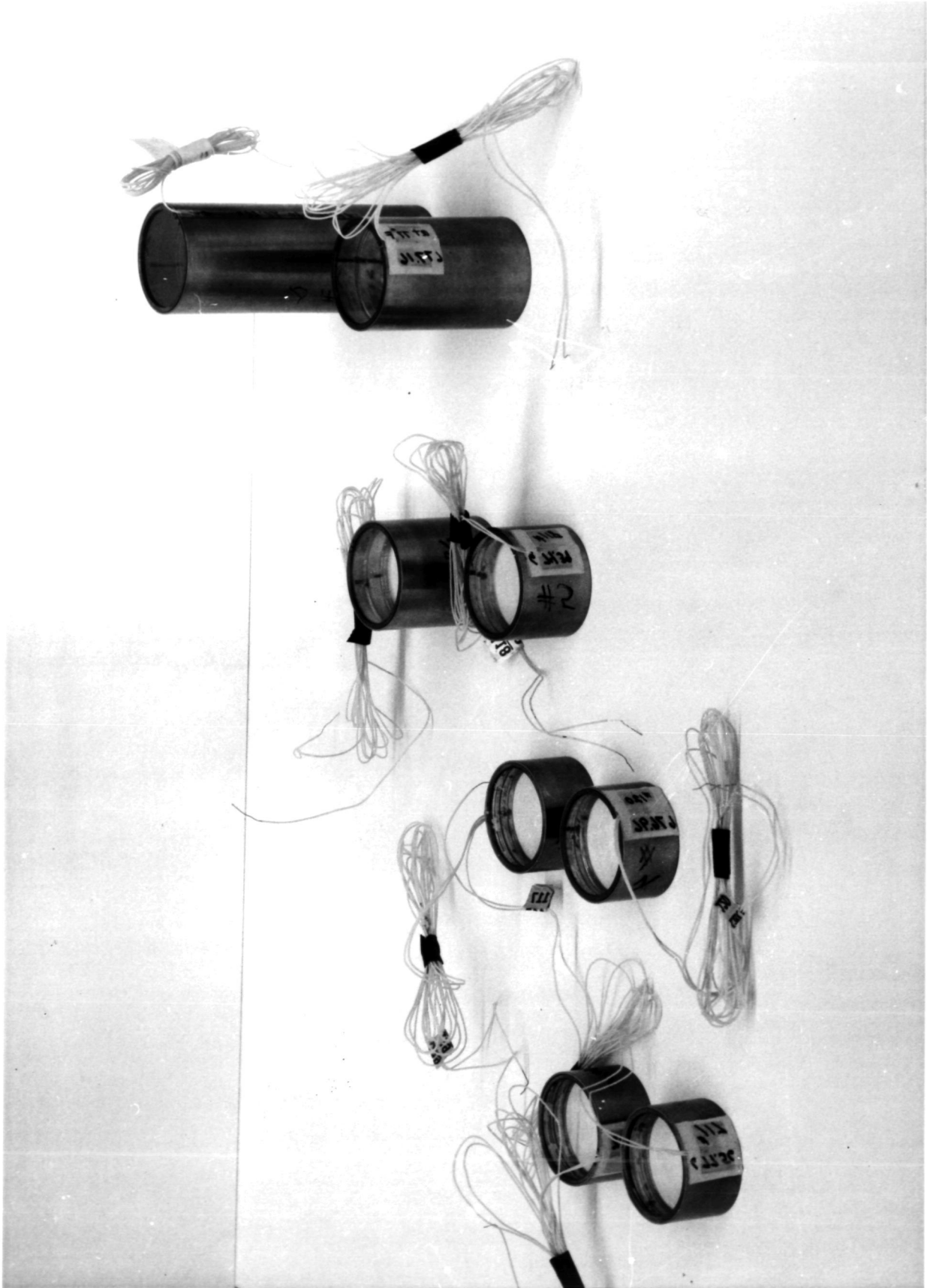


Figure 17



Figure 18

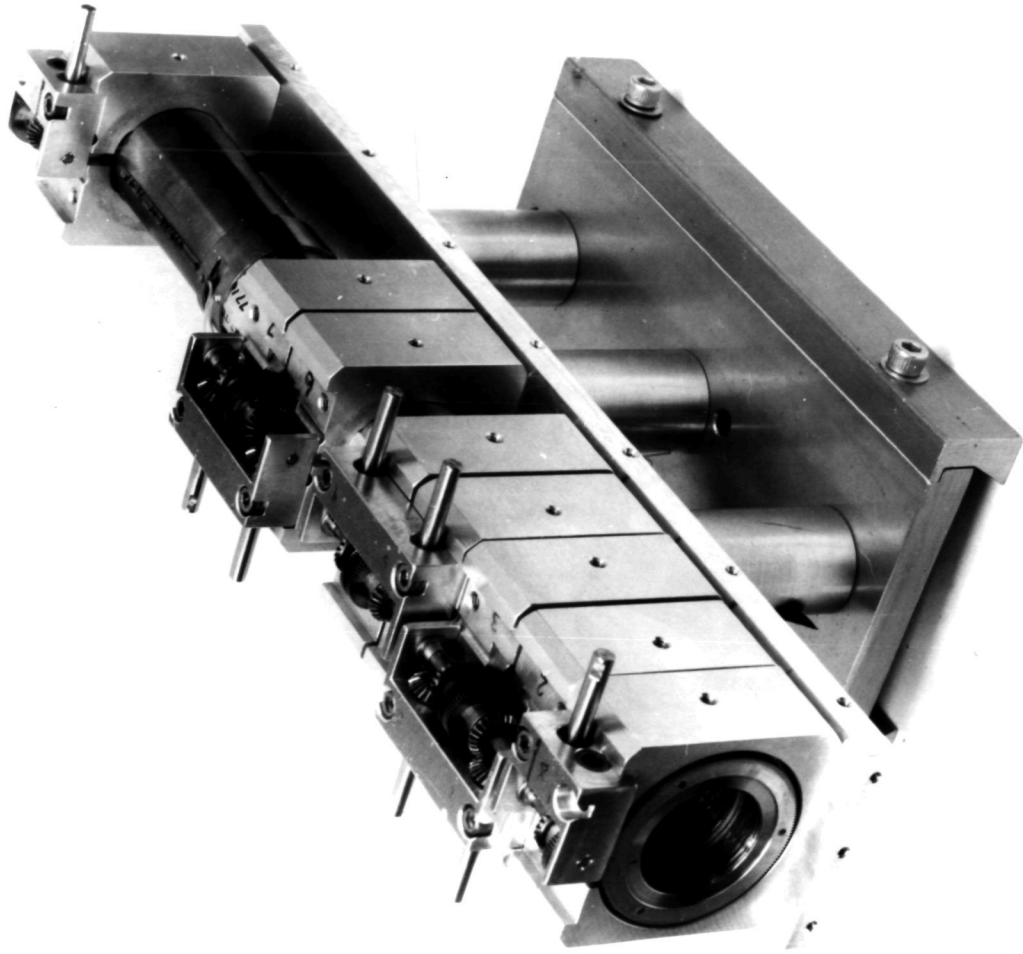


Figure 19

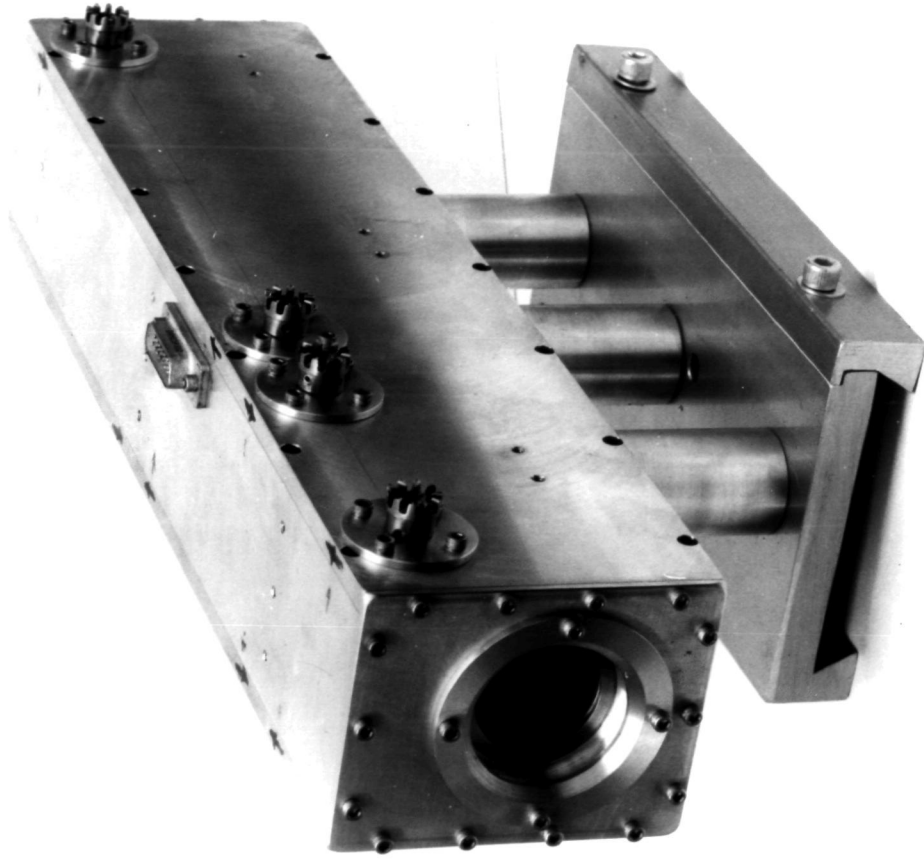


Figure 20

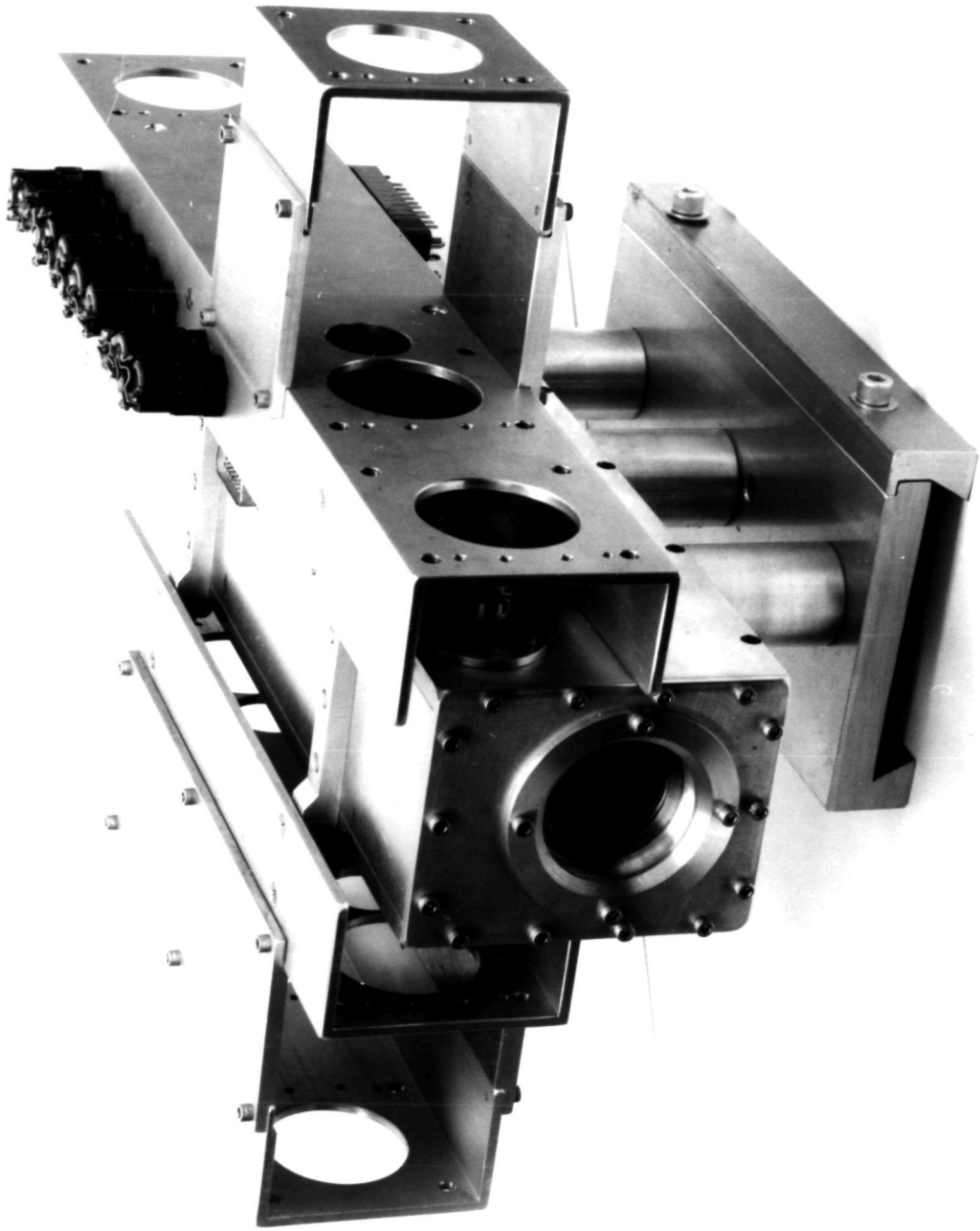


Figure 21

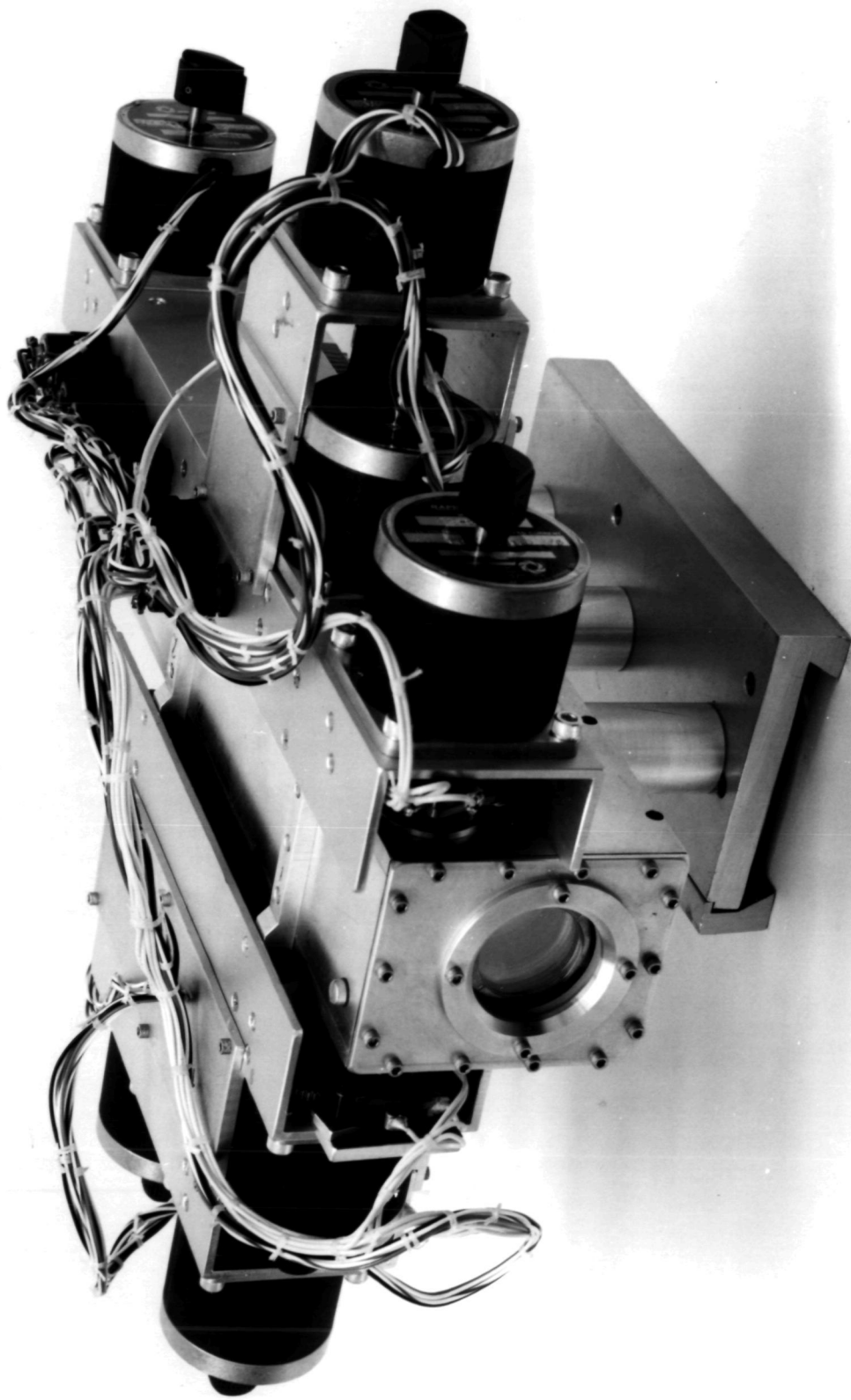


Figure 22

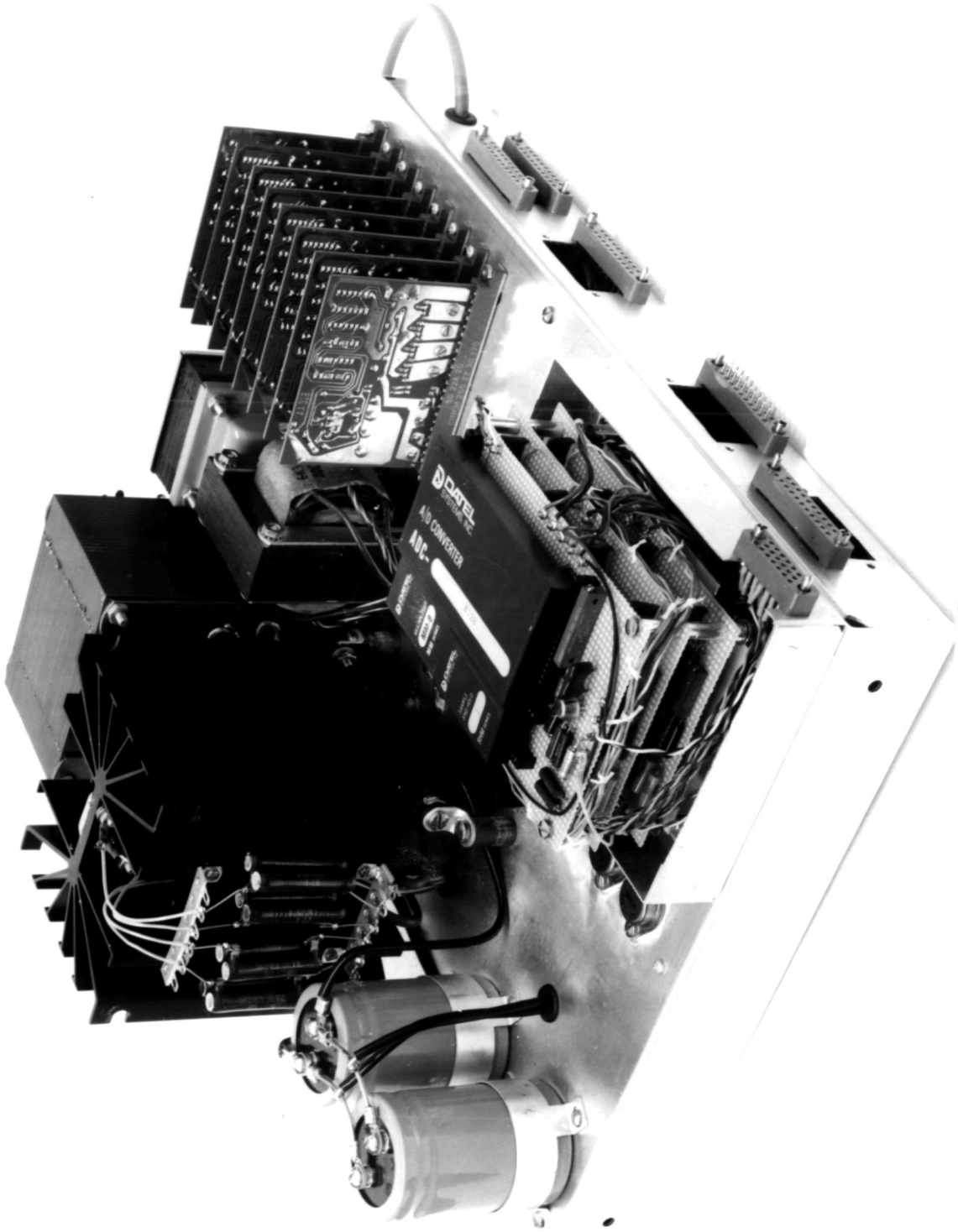


Figure 23

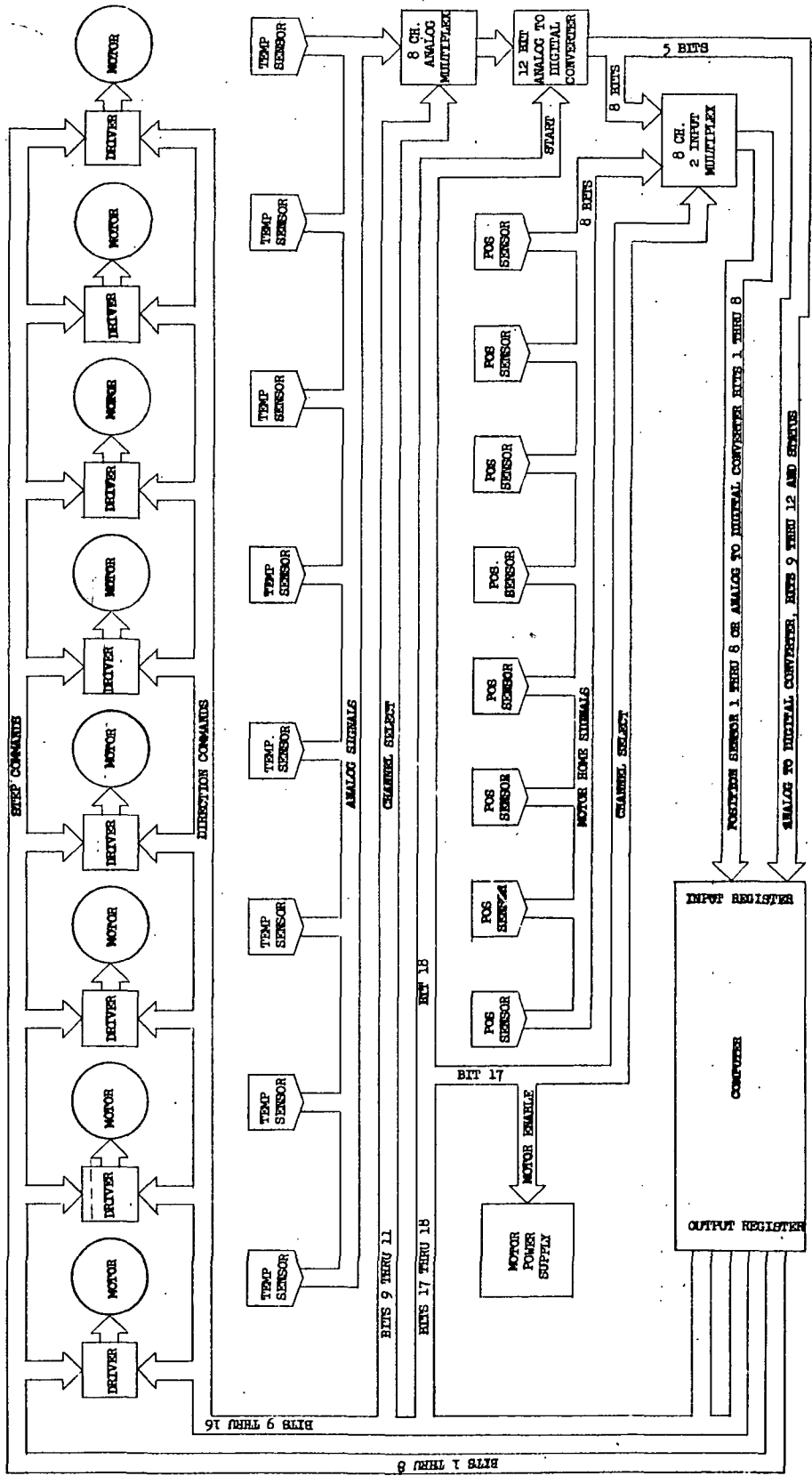


Figure 2a

COMPUTER I/O

OUTPUTS:

1	}	MOTOR STEP COMMANDS 1 THROUGH 8
2		
3		
4		
5		
6		
7		
8		
9	}	MOTOR DIRECTION COMMANDS 1 THROUGH 3, ANALOG MULTIPLEX CHANNEL SELECT
10		
11		
12	}	MOTOR DIRECTION COMMANDS 4 THROUGH 8
13		
14		
15		
16		
17 -		MOTOR ENABLE, 8 CH. 2 INPUT MULTIPLEX SELECT
18 -		ANALOG TO DIGITAL CONVERTER START COMMAND

INPUTS:

1	}	8 CH. 2 INPUT MULTIPLEX OUTPUT	}	POSITION SENSOR
2				OUTPUTS 1 THROUGH 8
3				IF OUT 17 HIGH
4				-----
5				ANALOG TO DIGITAL
6				CONVERTER BITS 1
7				THROUGH 8 IF OUT 17 LOW
8				
9	}	ANALOG TO DIGITAL CONVERTER BITS 9 THROUGH 12		
10				
11				
12	}	NOT USED		
13				
14				
15	}	ANALOG TO DIGITAL CONVERTER STATUS		
16 -				

Figure 25

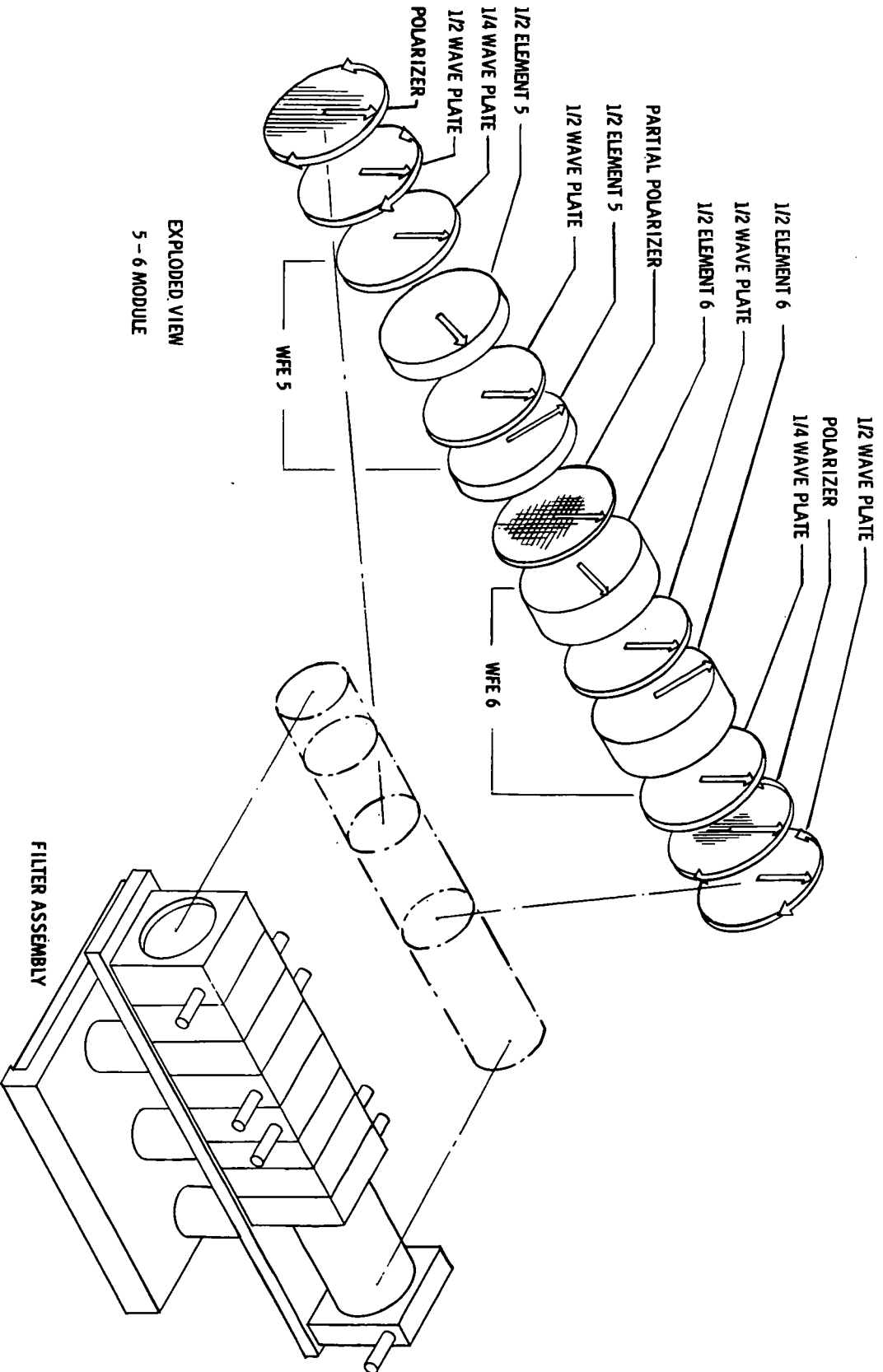


Figure 26

CHART 100-2113

CHART 100-2113

CHART 100-2113

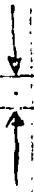
CHART 100-2113

5896

12



.111
(.1047)



116

115

Figure 27

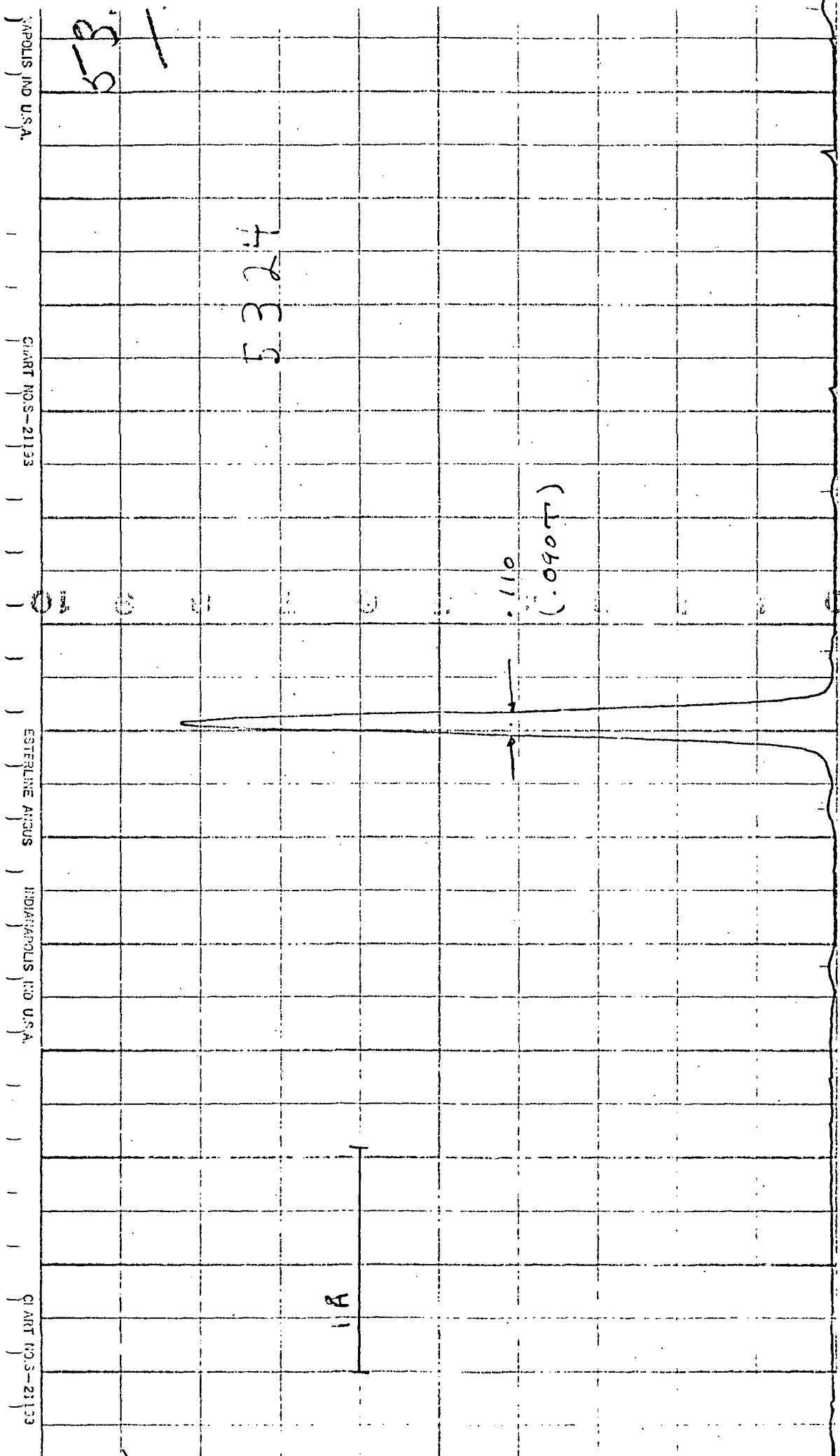


Figure 28

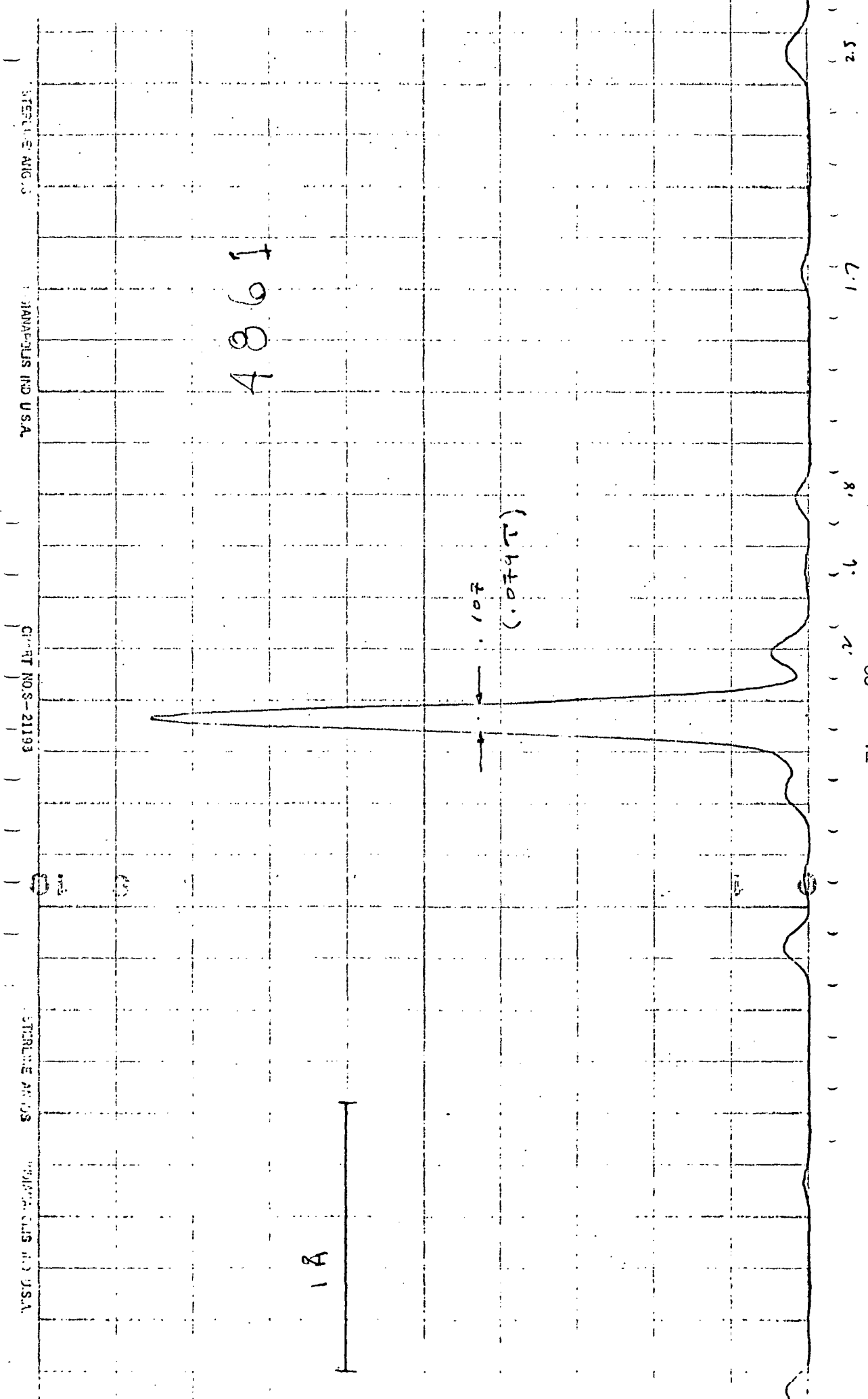


Figure 29

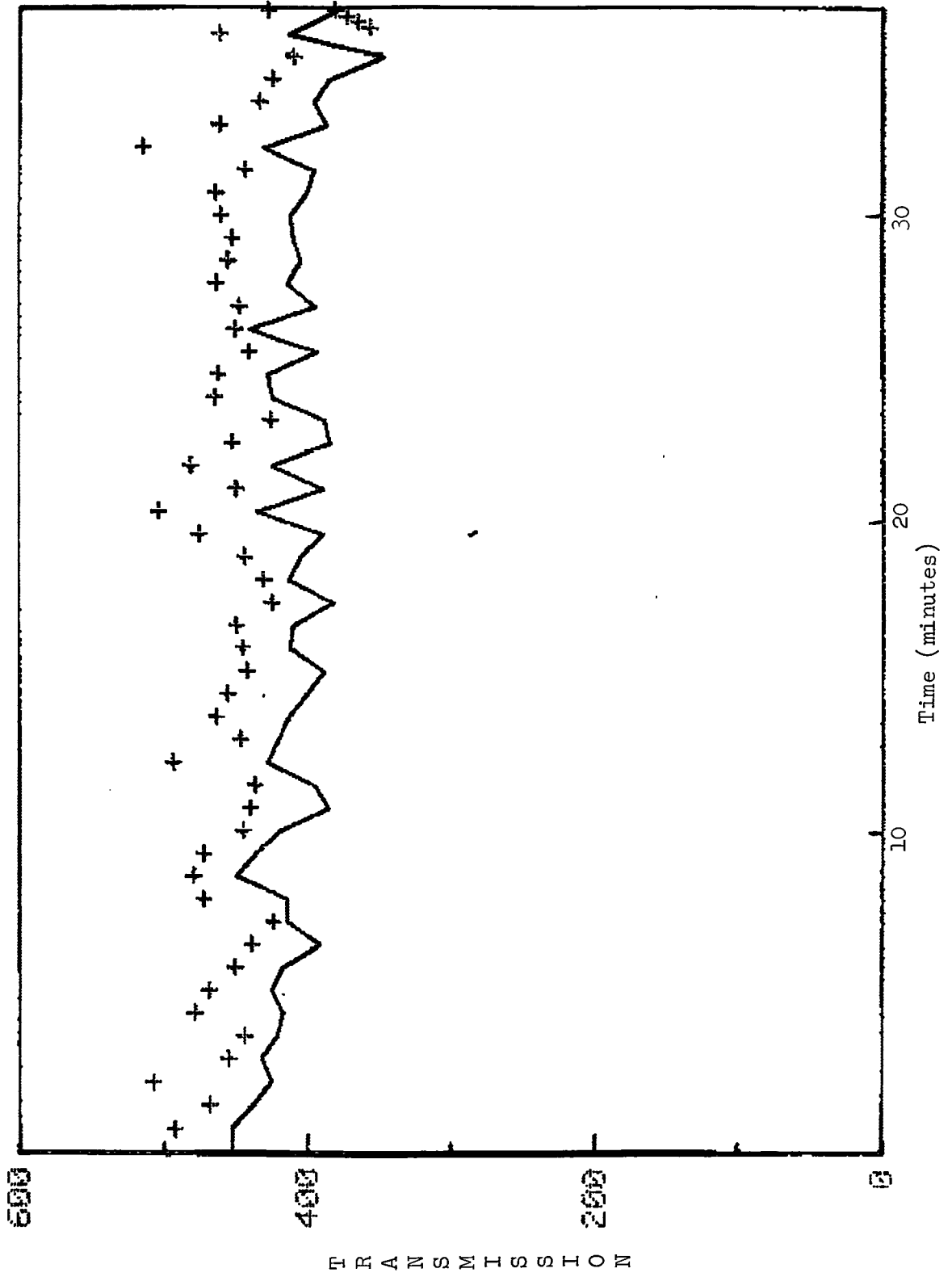
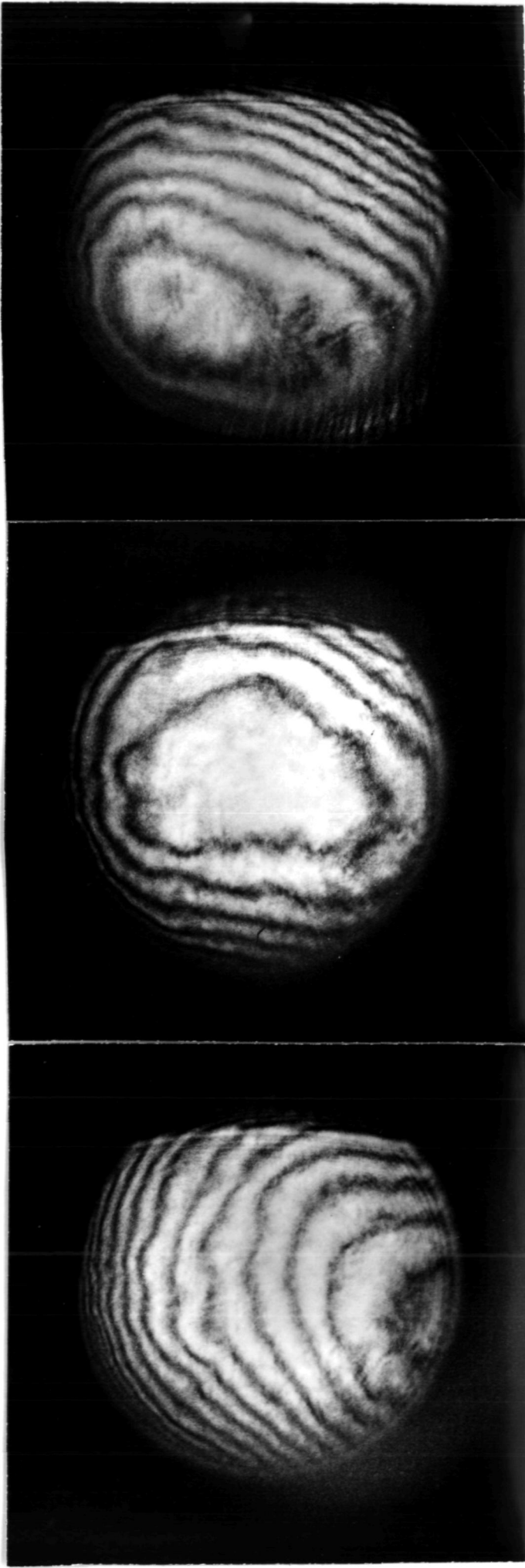


Figure 30



a) Reference mirror displaced in the vertical plane.

b) Reference mirror parallel to test optic.

c) Reference mirror displaced in horizontal plane.

Figure 31 LUPI Interferograms

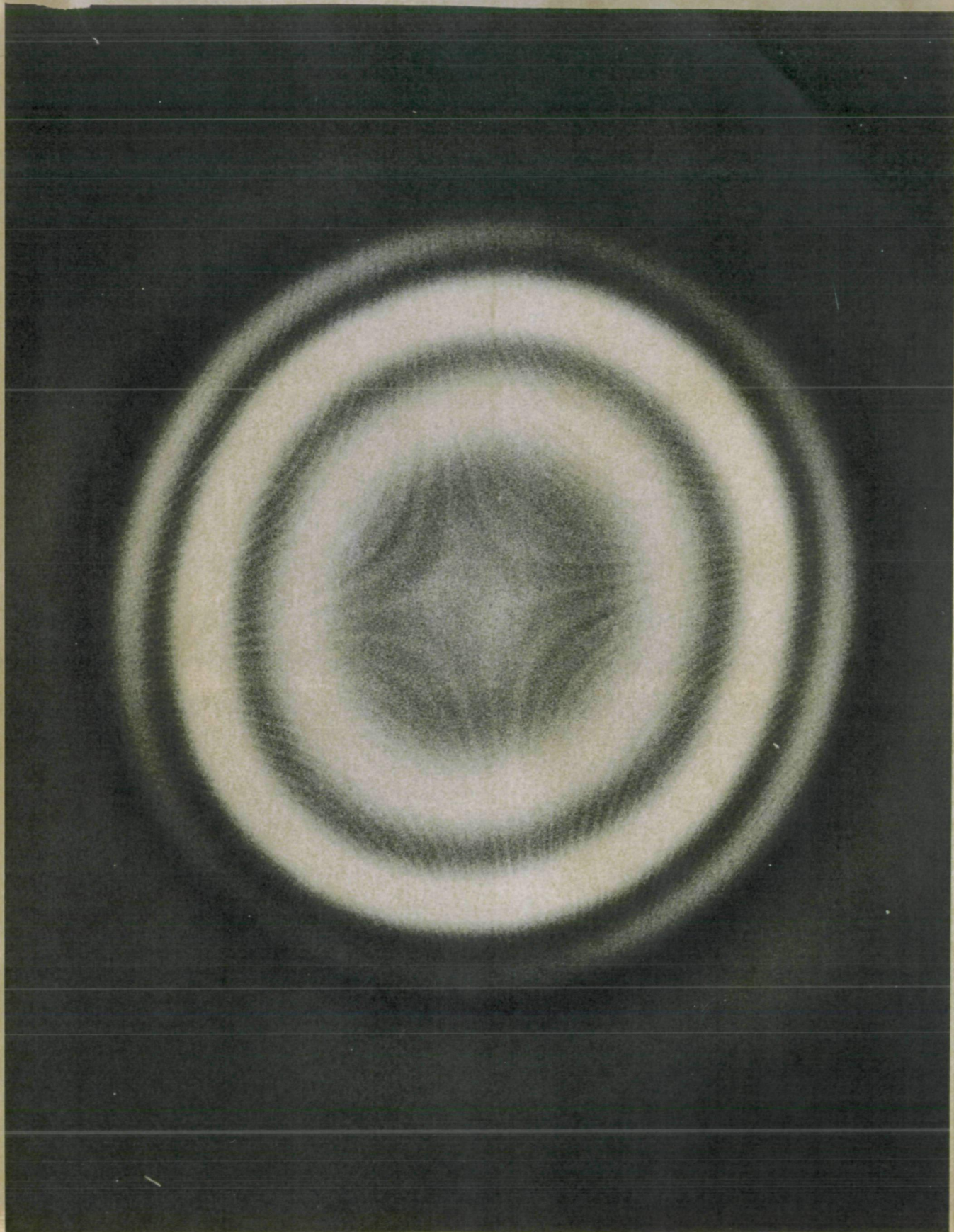


Figure 32